Australian Government
Geoscience Australia

Description, Distribution and Potential CO_2 Storage/Seal Capacity of the Cenozoic Sandstones and Carbonates

Browse Basin, Western Australia

Alanna Simpson and Michelle Cooper
With contributions from Alfredo Chirinos and Anna-Liisa Lahtinen

Record
2008/13

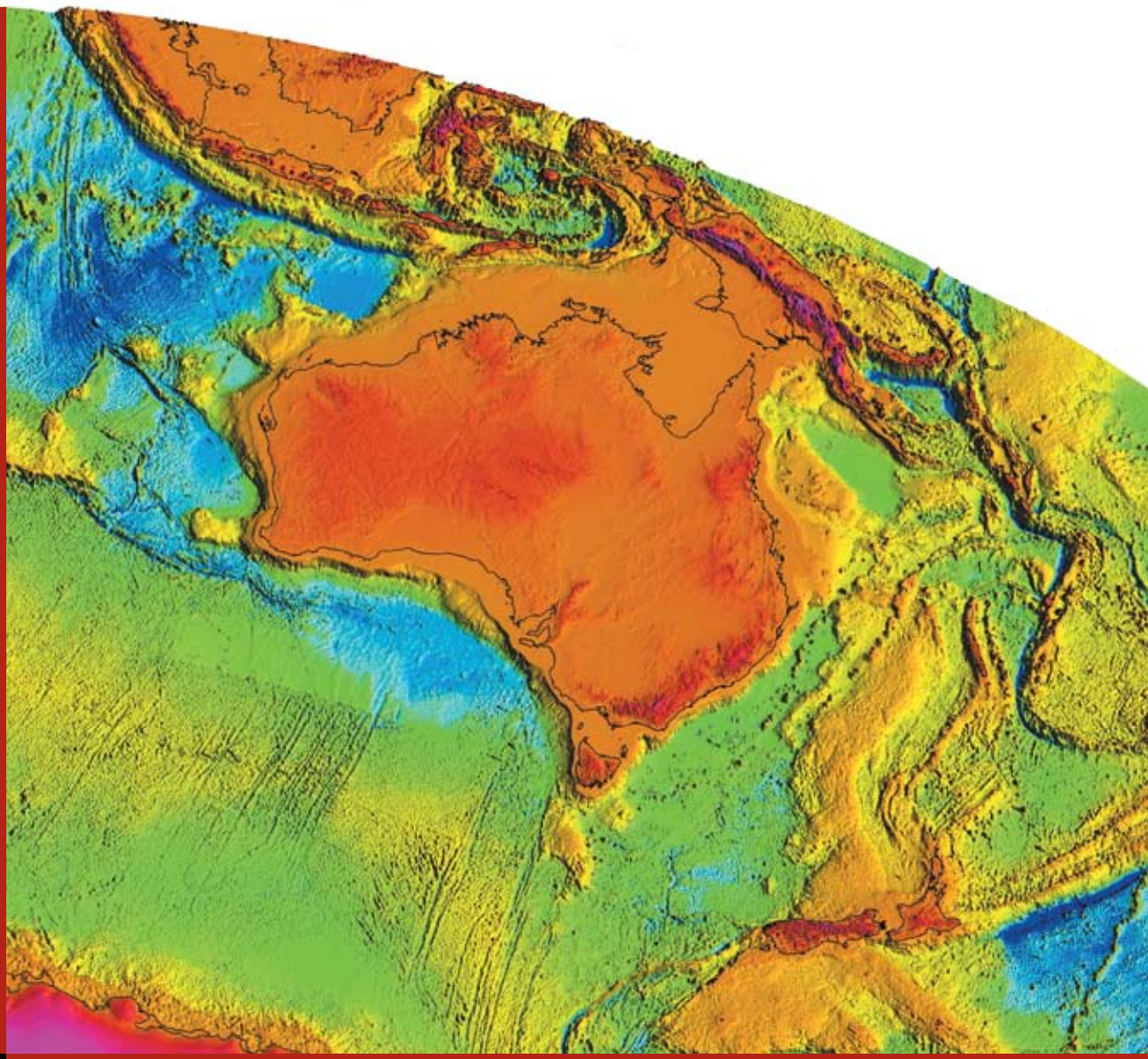

Description, Distribution and Potential CO_2 Storage/Seal Capacity of the Cenozoic Sandstones and Carbonates, Browse Basin, Western Australia

GEOSCIENCE AUSTRALIA
RECORD 2008/13

by

Alanna Simpson[1] and Michelle Cooper[1]

With contributions from Alfredo Chirinos[1] and Anna-Liisa Lahtinen[1]

Australian Government
Geoscience Australia

1. Geoscience Australia GPO Box 378 Canberra ACT 2601

Department of Resources, Energy and Tourism
Minister for Resources and Energy: The Hon. Martin Ferguson, AM MP
Secretary: Dr Peter Boxall, AO

Geoscience Australia
Chief Executive Officer: Dr Neil Williams PSM

ISSN 1448-2177
ISBN 978-1-921236-98-3 (Hardcopy)
ISBN 978-1-921498-00-8 (CD)
ISBN 978-1-921236-99-0 (Web)

GeoCat # 65933

Bibliographic reference: Simpson, A. and Cooper, M., 2008. Description, Distribution and Potential CO_2 Storage/Seal Capacity of the Cenozoic Sandstones and Carbonates, Browse Basin, Western Australia. Geoscience Australia, Record 2008/13. 51pp.

Contents

Executive Summary v

Introduction 1
Project Objectives and Tasks 1
Browse Basin Regional Geology 1
Browse Basin Development – Palaeozoic Through to the Cenozoic 2
Palaeographic reconstruction of the Browse Basin – Maastrichtian to Holocene 3

Project Methods 5
Well-Log Review and Quality Check 5
Cuttings Analysis 5
Geological Markers, Surfaces, Correlations, Regional Cross Sections and Palaeogeographical Maps 5
Seismic Signatures and Interpretation 6
Potential Geological Storage Capacity/CO_2 Storage Site Estimation 6
Database Quality Control 6

Cenozoic Sandstones 6
Introduction 6
Cenozoic Sandstone Distribution Within the Browse Basin 6
Cuttings Descriptions 7
Description and Classification Terminologies 8
Echuca Shoals-1 8
Copernicus-1 9
Discorbis-1 10
Bassett-1a 12
Caswell-2 13
X-Ray Diffraction (XRD) Analysis 14
Facies Analysis and Description of Wireline Log Response 14
Echuca Shoals-1 15
Copernicus-1 15
Discorbis-1 15
Bassett-1A 16
Caswell-2 16
Palaeoenvironmental Interpretation 17
Echuca Shoals-1 17
Copernicus-1 17
Discorbis-1 18
Bassett-1a 18
Caswell-2 18
Stratigraphic Boundaries 19
Echuca Shoals-1 19
Discorbis-1 19
Bassett-1a 19
Porosity and Permeability 20
Reservoir with the Highest Potential for CO_2 Storage in the Cenozoic Sandstone Section of the Caswell Sub-Basin 20

Cenozoic Carbonates 22
Introduction 22

Cenozoic Carbonate Distribution Within the Browse Basin....22
Carbonate Lithologies and Inferred Environments of Deposition....23
Description and Classification Terminology....24
Echuca Shoals-1....24
Copernicus-ST1....25
Discorbis-1....26
Bassett-1a....27
Caswell-2....29
Description of Wireline Log Response....30
Echuca Shoals-1....30
Copernicus-ST1....31
Discorbis-1....31
Bassett-1a....31
Caswell-2....31
Porosity and Permeability of the Cenozoic Carbonates....31
Palaeogeography of the Carbonates....34
Seal with the Highest Potential in the Cenozoic Carbonate Section of the Caswell Sub-Basin....35

Seismic Interpretation of the Cenozoic Sandstones and Carbonates....35
Paleocene (Tbase to Tpal)....39
Eocene (Tpal to Teoc)....40
Oligocene (Teoc to Tolig)....40
Early Miocene (Tolig to Temio)....41
Middle Miocene (Temio to Tmmio)....41
Late Miocene (Tmmio to Tlmio)....42
Pliocene to Holocene (Tlmio to Seabed)....43

Conclusions....44

Acknowledgements....45

References....45
Well Completion Reports....46

Appendices....47

Executive Summary

The Browse Basin is located in the southern Timor Sea region of Australia's North West Shelf and covers an area of ~140,000 km^2. It was identified as containing potential Environmentally Suitable Sites for carbon dioxide (CO_2) Injection (ESSCI) by the Australian Petroleum CRC's GEODISC program (1999-2003). A regional geological reconnaissance of Cenozoic sandstone and carbonate sequences in the Browse Basin was undertaken in 2007 to determine the potential storage and sealing capacity for geological storage of CO_2, the results of which are presented in this report. Methods included the review of available literature and well-completion reports, lithological and mineral analysis of selected well cuttings and interpretation of the wire-line and seismic response of the Cenozoic section.

Cenozoic sandstones are limited in distribution in the Browse Basin to the central and eastern basin with virtually no Cenozoic sandstones encountered in the north-western Caswell Sub-basin or Barcoo Sub-basin. This study therefore focussed on the central and eastern Caswell Sub-basin. Sandstones vary in thickness across the Caswell Sub-basin and while there is no clear gradient, as a general rule sandstone sequences are thinner (<350 m) towards the eastern and northern edges of the Sub-basin and thicker (most >600 m) towards the centre. Although the majority of Cenozoic sandstones encountered within the Sub-basin have generally good porosity, the sandstones located at depths >800 m (at P and T conditions required to maintain the supercritical state of CO_2), are found mostly through the central and northern Caswell Sub-basin.

The potential capacity of the Cenozoic carbonates within the Caswell Sub-basin to act as a seal for underlying reservoir sandstones was evaluated using lithological properties (e.g. composition, porosity), thickness, palaeographic reconstructions and Mercury Injection Capillary Pressure (MICP) testing. MICP analysis of carbonate cuttings, collected from across the Caswell Sub-basin, reveals that samples with a high micritic component (e.g. calcareous mudstones) and well-cemented to recrystallised grainstones have the best potential seal capacity of the observed carbonate lithologies.

Based on the geographical distribution of the various facies types and on the thickness of the carbonate interval, the central Caswell Sub-basin has the highest potential for geological storage of CO_2. Here, a reservoir thickness of >1300 m and a 600 m thick sequence of packstones and wackestones with relatively low porosity (visual porosity from mudlogs), represents a potentially good reservoir/seal pair for CO_2 storage. Furthermore, palaeogeographic reconstructions indicate that this area did not experience significant erosion or long-term aerial exposure during several Cenozoic lowstand periods, thus the probability of secondary porosity development or karstic features within these carbonates is relatively low. The region surrounding wells Caswell-2 and Walkley-1 has the highest quality Cenozoic reservoir and seal pair observed in the basin and importantly also appears to lack the recent faulting that is typical of the north-eastern Caswell Sub-basin.

Introduction

A regional geological reconnaissance of Cenozoic sandstone and carbonate sequences in the Browse Basin, located offshore off the north-west coast of Western Australia, was undertaken to determine prospective CO_2 locations for geological storage of carbon dioxide (CO_2), including an assessment of the sealing capacity potential of the overlying carbonate sequence.

Previous work by the Australian Petroleum CRC's (APCRC) Geological Disposure of CO_2 (GEODISC) program, established the feasibility of CO_2 injection and storage in Australian sedimentary basins (Bradshaw & Rigg, 2001). Subsequent research undertaken at Geoscience Australia and the Cooperative Research Centre for Greenhouse Gas Technologies (CO2CRC) has advanced knowledge of these sites including assessment of their potential as Environmentally Suitable Sites for CO_2 Injection (ESSCI). Potential CO_2 storage locations have been recognised in the Browse Basin, consequently, this report aims to further evaluate the Cenozoic sandstone and carbonate sequences as a potential storage reservoir and seal, respectively.

Project Objectives and Tasks

The overall objectives of this study was to review and collate previous work and, where required, make new observations on the lithology, reservoir properties and lateral and vertical extents of the Cenozoic sandstones and carbonates in order to determine their potential for CO_2 storage. To achieve this objective the following distinct tasks were identified:

- Review and synthesise the depositional histories of the Cenozoic sandstones and carbonates.
- Identify the respective seismic signatures of the sandstones and carbonates.
- Integrate well and seismic data to construct regional cross sections and produce palaeogeographical maps (log signature/depositional environment) and describe the lateral and vertical distribution of the sandstones and carbonates in the basin.
- Sample well cuttings throughout the basin and where possible send carbonate samples for seal capacity evaluation.
- Based on the distribution and reservoir properties of the sandstones and carbonates, ascertain which areas within the Browse Basin Cenozoic Sequence have the highest potential for CO_2 storage.

Browse Basin Regional Geology

The Browse Basin is located in the southern Timor Sea region of Australia's North West Shelf and covers an area of ~140,000 km^2 (Figure 1). The Browse Basin comprises four major Sub-basins: the Caswell, Barcoo, Scott and Seringapatam Sub-basins, and is bordered to the south-east by shallow basement (the Prudhoe Terrace, Yampi and Leveque shelves) (Stephenson & Cadman, 1994). The Caswell Sub-basin, a focus of this study, is the major depocentre of the Browse Basin containing up to 20 km of Palaeozoic to Cenozoic sediments. The following section briefly discusses the Palaeozoic to Cenozoic evolution of the Browse Basin with more detail provided on its Cenozoic history.

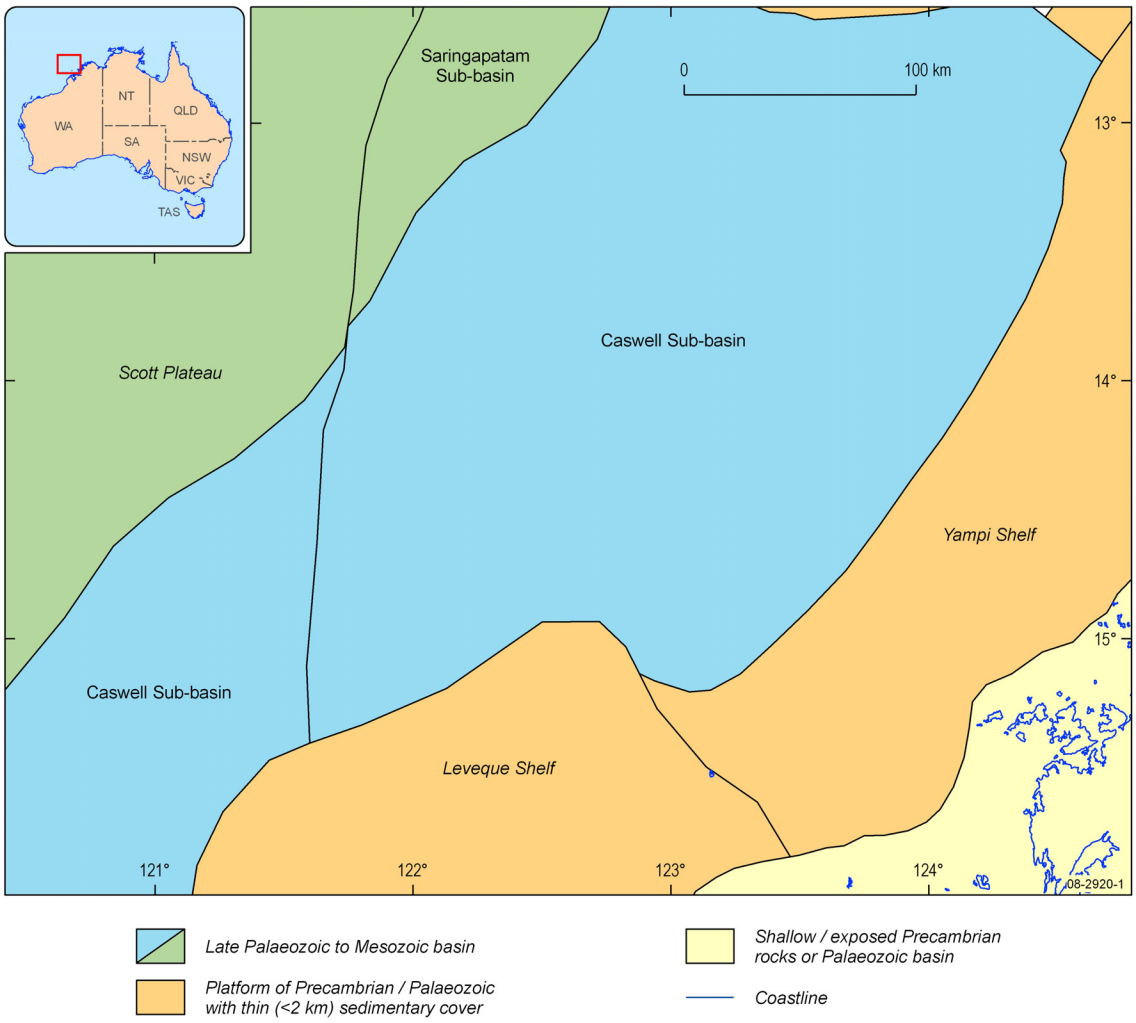

Figure 1: *Browse Basin regional structural elements map (from AGSO Browse Basin Project Team, 1997; Blevin et al., 1998, Struckmeyer et al., 1998).*

Browse Basin Development – Palaeozoic Through to the Cenozoic

The Browse Basin shows evidence of a multi-stage deformational history with six major basin phases delineated in the Browse Basin High Resolution (BBHR) study, which includes two cycles of extension, thermal subsidence and inversion (AGSO *Browse Basin Project Team*, 1997; Blevin et al., 1998, Struckmeyer et al., 1998). These tectonic events are summarised in Figure 2 and below.

Late Carboniferous to Early Permian extension: Extension within basin during this time produced a series of half grabens and the distinct Sub-basins of the Browse resulted from large-scale normal faulting. This extension is marked by a transition from fluvio-deltaic deposition in the Carboniferous to a typically marine environment in the Early Permian.

Late Permian to Triassic thermal subsidence: During this period there was extensive deposition of shallow marine to passive margin shelfal carbonates and mixed clastics, up to 5 km in thickness. The period of deposition was accompanied by thermal subsidence. Sediments from this basin phase are characterised by a transgressive cycle of clastics overlain by carbonates.

Late Triassic inversion: Deposition was terminated and a regional unconformity formed near the top of the Triassic section due to inversion of Palaeozoic half grabens. This event led to the widespread formation and subsequent erosion of anticlinal and synclinal structural features.

Early Jurassic extension: In contrast to the Late Carboniferous extensional event, extension in the Early Jurassic was accommodated by numerous relatively small normal faults. Movement along these faults caused the collapse of the Late Triassic anticlinal features. Fluvial and deltaic-to-shallow marine clastics in the east and distal marine shales in the west filled the newly formed half graben.

Late Jurassic to Cenozoic thermal subsidence: Widespread deposition followed the end of rifting and sediment loading exacerbated thermal subsidence. Minor reactivation of faults occurred in the latest Jurassic through to the Late Cretaceous. Prograding and transgressive sediments of the Late Jurassic are truncated by a major erosional surface on top of the Late Jurassic highstand facies. Aggradation and progradation in the Cretaceous produced sand and shale sequences and in the latest Cretaceous transgressive carbonates, fluvio-deltaic and prograding siliciclastics sequences were deposited and valleys were incised.

Middle to Late Miocene inversion: The most recent structural events within the Browse Basin occurred in the Middle to Late Miocene due to the collision of the Australian tectonic plate with the Eurasian plate. In the Caswell Sub-basin, the Miocene inversion was typically confined to small-scale extensional faults; however, in the north of the Sub-basin considerable fault offsets formed during this period.

Palaeographic reconstruction of the Browse Basin – Maastrichtian to Holocene

A palaeographic study of the Browse Basin by Stephenson and Cadman (1994) includes reconstructions of three periods within the Late Cretaceous and Cenozoic. These are summarised below:

Late Cretaceous to Early Paleocene: Towards the end of the Cretaceous, subsidence rates within the Browse Basin were overtaken by progradation of a carbonate wedge in the north. This is illustrated at Caswell-2 where middle to outer shelf sediments are overlain by inner- to middle-shelf shale and sandstone. A significant feature of the Paleocene shelf progradation is the sandy nature of the sediments. The speed of the progradation is reflected in the northern Caswell Sub-basin where upper continental sediments rapidly change to inner-continental shelf sediments.

Eocene to Oligocene: During this period basin subsidence overtook shelf progradation, resulting in deeper water in the central basin. Caswell-2 now lay in the outer shelf; thus inner- to middle-shelf shales and sandstones are overlain by outer-shelf carbonates. Bassett-1a, Echuca Shoals-1 and Heywood-1 also show evidence of deeper waters with deposition of middle-shelf, inner-shelf, and marginal-marine-to-fluvial-deltaic sediments, respectively. During the middle Oligocene a major drop in sea level, recognised globally, resulted in local non-deposition or erosion in the Browse Basin. Evidence of this shallowing is recognised at Scott Reef-1 where middle- to outer-shelf carbonates are overlain by inner-shelf carbonates.

Miocene to Holocene: Open marine conditions have continued to the present day except for relatively short-term exposure of part of the continental shelf during the Pleistocene glacial maxima. Whilst short-term fluctuations in water depth and sediment facies are recognised to have occurred in this time period, the authors believe that there is insufficient data for further palaeographic reconstructions.

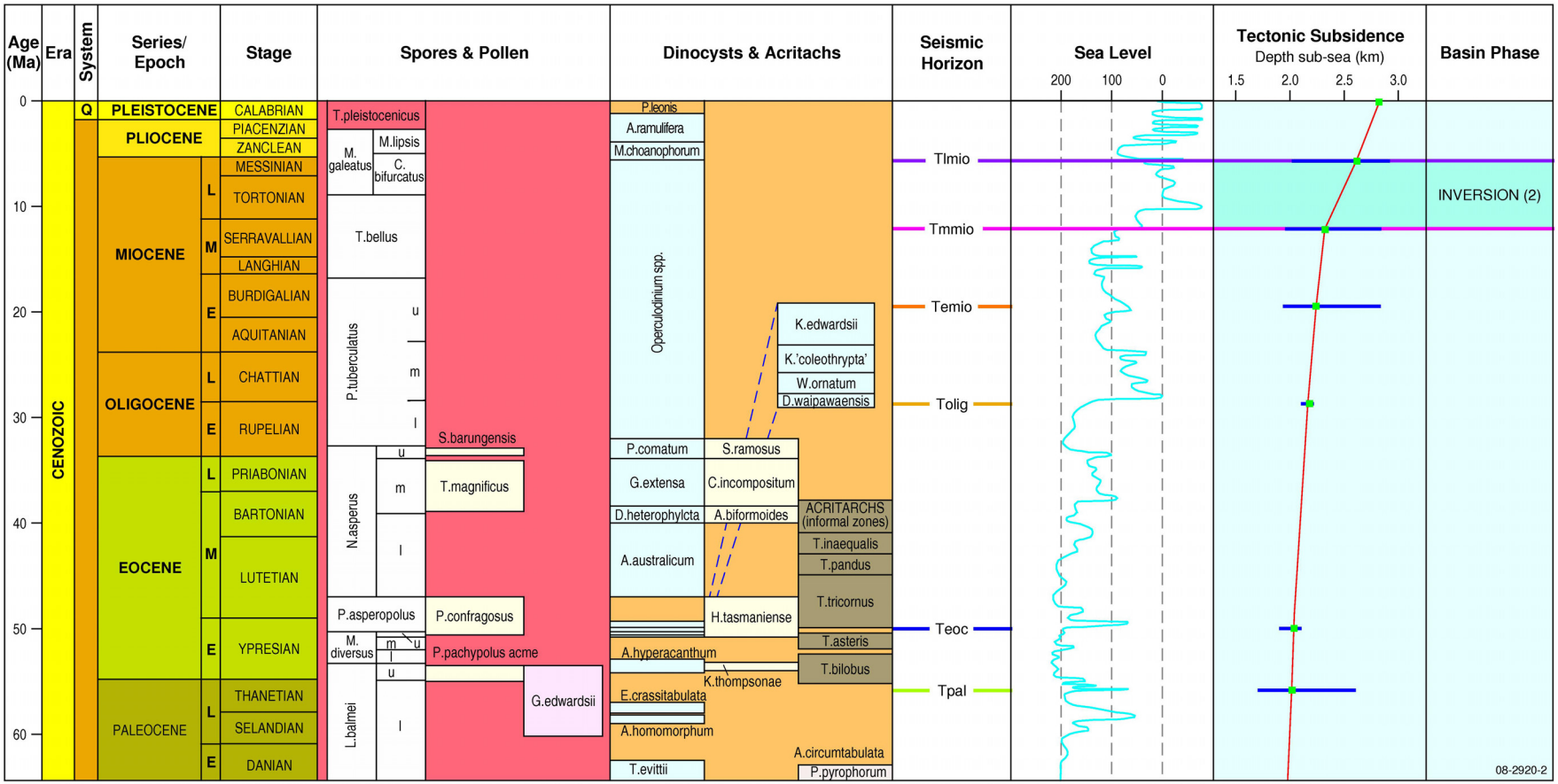

Figure 2: *The timescale, biozonation, and stratigraphic data relevant to the Browse Basin were compiled using Timescale Creator Pro 1.2 and using the GTS 2004 Timescale .Sea level date from Hardenbol, J., et al (1998).*

Project Methods

The following section provides details on the techniques used in this study.

WELL-LOG REVIEW AND QUALITY CHECK

A spreadsheet detailing key information about the Cenozoic sequences, such as depth to carbonate sandstone contact and sequence thicknesses, was compiled and is presented in Appendix A1. Although all wells in the Barcoo and Caswell Sub-basins are included on the well-descriptions spreadsheet, the initial well log examination revealed that Cenozoic sand units were extremely thin to non-existent in the Barcoo Sub-basin. Consequently, detailed stratigraphy was only compiled for wells in the Caswell Sub-basin that contain sandstones, and were further prioritised to those with cuttings available for analysis.

CUTTINGS ANALYSIS

Five wells were selected in the Caswell Sub-basin for detailed cuttings analysis upon completion of the well-log review and quality check: Echuca Shoals-1, Copernicus-1, Discorbis-1, Bassett-1a and Caswell-2. The Cenozoic units were not cored in any of the wells in this study and so this analysis is based upon cuttings. The selected wells fulfilled the following criteria: carbonate and sandstone cuttings were recovered; the top of the sandstone sequence was below 800 m depth; and the selected wells provided the greatest spatial coverage of the Sub-basin. The map in Figure 3 highlights the selected wells and the wells for which detailed well summaries are provided in Appendix 1.

To select the cuttings for microscopic examination the second or third cutting (10 to 20 m intervals) in each well was laid out for viewing. Changes in colouration, grain size or content were noted and samples were selected at significant transitions and from representative parts of the section. Samples were also examined if a distinct change in the gamma ray or sonic log response was observed. Finally, multiple samples were chosen from sections that appeared particularly homogeneous (visually and in the wireline log response) to ensure that any changes in these sections were identified.

Samples were examined and photographed under the microscope and the grain size, sorting, shape, colour and lithology of the sample were recorded. The approximate proportions of minerals were noted and for carbonate samples the proportion of skeletal material, calcareous clay/silt (micrite) and calcite grains were recorded providing the basis for a preliminary carbonate rock classification (see Carbonate Section). These details were recorded in a spreadsheet (Appendix 2 and 3) and summaries are presented in the relevant sections of this report

Approximately 10 g samples from a selection of carbonate cuttings were collected and submitted for Mercury Injection Capillary Pressure analysis (MICP; seal capacity testing for carbonate samples) or X-Ray Diffraction. Further details of MICP analysis are given on Australian School of Petroleum website: http://www.asp.adelaide.edu.au/research/micp/background/ and Appendix 4.

GEOLOGICAL MARKERS, SURFACES, CORRELATIONS, REGIONAL CROSS SECTIONS AND PALAEOGEOGRAPHICAL MAPS

Well-cutting descriptions were combined with wireline logs (gamma ray and sonic) to construct regional cross sections and palaeogeographic maps that provide constraints on the lateral and vertical distribution of the sandstones and carbonates in the basin. GeoFrame software was used to generate cross-sections containing Browse Basin High Resolution seismic survey (BBHR) geological time boundaries. These boundaries were compared to those in the well completion reports.

SEISMIC SIGNATURES AND INTERPRETATION

Five seismic lines intersecting the five selected wells were selected for examination from the available BBHR survey lines with the selection providing a broad spatial coverage of the Caswell Sub-basin. Four lines traverse SE to NW, from inner shelf to outer shelf while the fifth line provides an intersection running from SW to NE through the centre of the basin (see Seismic Modelling section, Figure 18, page 36). The lithology determined from well cuttings or well-completion reports was correlated with seismic lines.

POTENTIAL GEOLOGICAL STORAGE CAPACITY/CO_2 STORAGE SITE ESTIMATION

Recommendation of potential CO_2 storage sites is based upon reported porosity and permeability, lithology, palaeogeography, unit thickness and structural integrity indicated by the presence or absence of Cenozoic deformation in both sandstone and carbonate units.

DATABASE QUALITY CONTROL

An effort was made to ensure consistency across both existing and new databases and spreadsheets. While collating wireline log data, cuttings lithology and seismic horizon information, discrepancies in the allocation of time horizons within a number of wells were discovered. These are discussed in more detail in a later section.

Cenozoic Sandstones

INTRODUCTION

The Cenozoic sandstones of the Browse Basin have mostly remained under-investigated in the search for oil and gas. Exploration activities have targeted Permian to Mesozoic formations and as such, the description, analysis and interpretation of younger sequences has not been a priority. However in the new world of carbon dioxide capture and storage, the sandstones of the Cenozoic provide an attractive potential reservoir for geological storage of CO_2. In this study the potential of the Cenozoic sandstones of the Browse Basin to store CO_2 and the distribution and character of the sandstones have been investigated, and a palaeoenvironmental interpretation has been completed using a number of available resources: well completion reports, selected well cuttings and wireline logs. Later in this report, combined with similar information about the potential Cenozoic carbonate seal, seismic modelling will be used to examine depositional features, unconformities, unit thickness and clastic versus carbonate depositional boundaries. Ultimately a site that provides the best potential for geological storage within the central Browse Basin will be identified.

CENOZOIC SANDSTONE DISTRIBUTION WITHIN THE BROWSE BASIN

Initial examination of well completion reports at the commencement of this project quickly showed that although there are significant thicknesses of Cenozoic carbonates present within both the Barcoo Sub-basin and the Caswell Sub-basin, in the Barcoo, Cenozoic sandstones are extremely rare to absent. This is also true of the Cenozoic sandstones in the north-western section of the Caswell Sub-basin. As a result, no further investigation of wells in the Barcoo was undertaken.

Within the remainder of the Caswell Sub-basin, sandstone thicknesses vary from less than 100 m on the eastern edge to over 1100 m towards the centre of the basin. Although there is no clear gradient, as a general rule sandstone sequences are thinner (<350 m) towards the eastern and northern edges of the Sub-basin and thicker (most >600 m) towards the centre (Figure 3). However sandstone thicknesses can vary quite sharply even between wells that are in close proximity to each other (e.g.

Caswell-2 and Walkley-1 are located approximately 50 m apart, 935 m and 473 m of Cenozoic sands respectively). The reason for this difference was not determined in the course of this research.

It is important to note that although the Cenozoic sediments are predominantly sandy sequences overlain by carbonates, sands are often interbedded with carbonates, particularly in the northern and eastern parts of the Caswell Sub-basin.

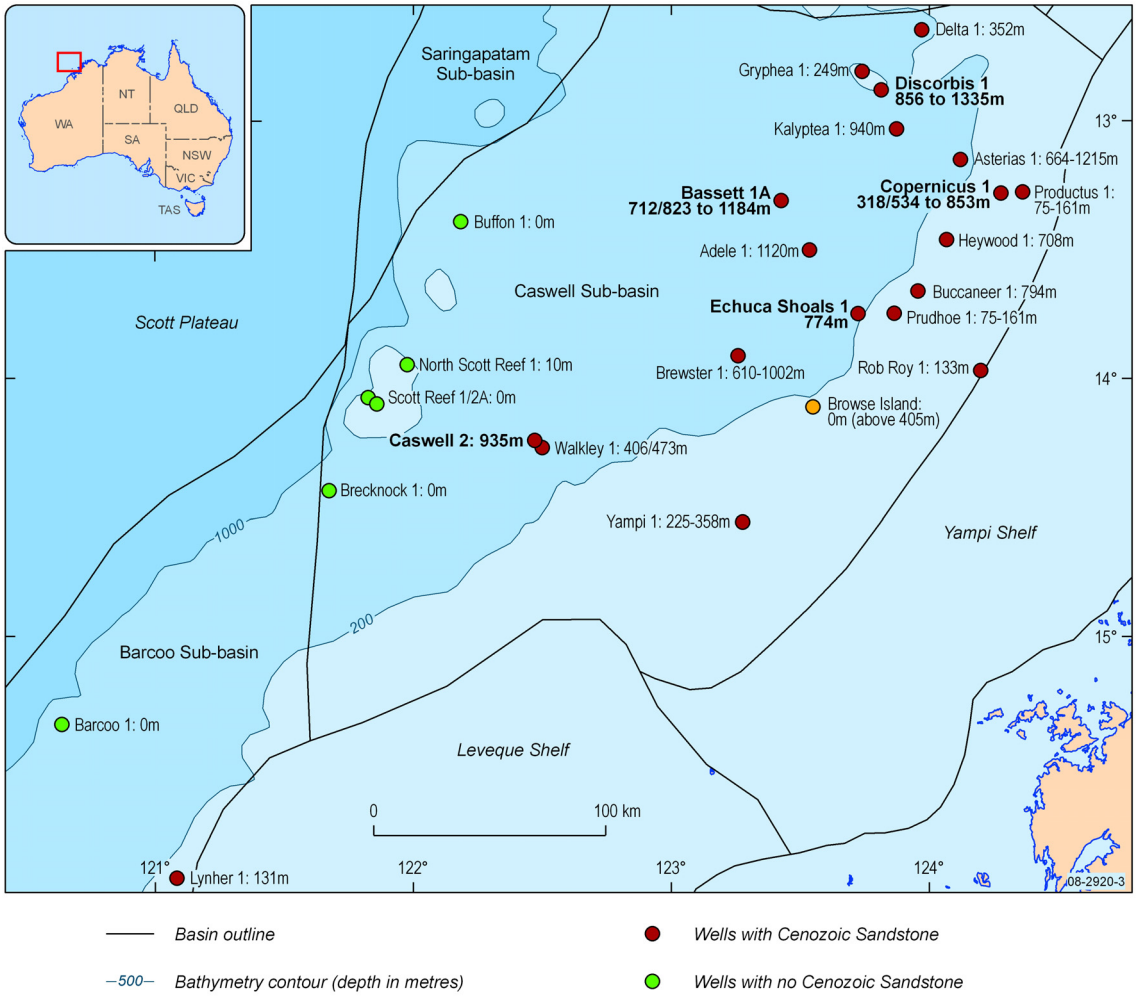

Figure 3: *Cenozoic sand distribution and thickness within the Caswell and Barcoo Sub-basins.*

CUTTINGS DESCRIPTIONS

Examination of cuttings from the Cenozoic sand sequences in Discorbis-1, Copernicus-ST1, Bassett-1a, Echuca Shoals-1 and Caswell-2 (Figure 3) was carried out to determine lithology, investigate palaeoenvironment and quality check well completion reports.

The descriptions presented in this section are lithological summaries of the cuttings examined, beginning in the late Maastrichtian or Early Cenozoic for each well; full cuttings descriptions can be found in Appendix A2. As there are some discrepancies between the well completion reports and the BBHR seismic survey regarding the location of the Mesozoic – Cenozoic stratigraphic markers, the stratigraphic boundaries referred to in the following cuttings descriptions are those assigned by the BBHR seismic survey.

Description and Classification Terminologies

The terminology used to describe the sandstones and carbonates differs between well completion reports; this section details the terminology used in the subsequent descriptions. Descriptions of sorting conform to the Compton classification (Compton, 1962) while grain shape (angularity/roundness) determination was based on the AMSTRAT (American/Canadian Stratigraphic) size-class comparison classes.

It must also be noted that the term sandstone in this context refers to quartz/clastic sands unless otherwise described. It is worth nothing that while overall the following cuttings descriptions concur with the lithology described in well completion reports, in detail there are often minor inconsistencies. For example the report for Copernicus-1 states that between 1065-1136 m RT the grain size becomes increasingly smaller, a fact not borne out in our examination of cuttings.

Grain size was determined using the Udden & Wentworth Scale (Wentworth, 1922) and has been used to describe grains greater than 0.062 mm in diameter. Grains that were discernable but of indeterminable size have been described as clay/silt highlighting the distinction made between fine but visible grains and ultra-fine cements. Clay/silt was most commonly observed as clasts that range up to 1 cm in size but was also unconsolidated in a number of samples. A distinction was also made between calcareous clay/silt and non-calcareous clay-silt. Observations of quartz grain colour were made and recorded in the cuttings spreadsheet (Appendix 2): clear/cloudy describes clear to translucent grains, white indicates that the grain was opaque; other colours are clear to cloudy unless described otherwise.

General carbonate descriptions refer to calcite and unless described otherwise, colour refers to opaque grains. When describing dolomite grains, unless noted otherwise, the colour refers to clear/cloudy grains. For both calcite and dolomite grains ‘finely crystalline’ describes crystal sizes between 30 μm and 1 mm while ‘coarsely crystalline’ refers to crystal sizes greater than 1 mm. Skeletal fragments were noted in a number of samples and their presence is also noted in sample descriptions. Carbonate rock classifications were approximated using a modified form of the Dunham classification system summarised in Table 1 and described in the Carbonate section. The mineral proportions within each cutting were estimated to provide a relative comparison between samples.

Finally, a number of additional minerals are present within the cuttings: glauconite (in both sandstones and carbonates, particularly dolomite) and an oxidised iron mineral (ankerite/siderite) are common. Although glauconite can be considered diagnostic of continental shelf depositional environments with low rates of accumulation, or develop as a consequence of diagenesis, no effort has been made here to attribute it to a type of depositional environment or aid in an interpretation of diagenetic processes.

Echuca Shoals-1

Cuttings from the Echuca Shoals-1 well were collected every 5 m from within the Cenozoic sand section. Between 830 m and 1690 m, 28 cuttings were examined and selected photomicrographs of the sediments can be seen in Figure 4.

The late Maastrichtian sediments in Echuca Shoals-1 consist of interbedded siltstone/shale and sandstone, muddy below 1590 m. Above these lies medium to coarse-grained sandstone, that becomes increasingly well-sorted with decreasing depth, with a layer of siltstone at 1512 m. Immediately below the Cenozoic – Maastrichtian boundary are two layers of organic/coal-rich material and sandstone (Figure 4b), separated by a clean sand layer.

The Paleocene is represented by an approximately 245 m thick package of relatively clean, coarse to medium-grained sandstone that varies from sub-angular to rounded, and from moderate to well to poorly sorted with decreasing depth. Only one sample was examined from the 73 m thick Eocene sequence. It was composed of clean, moderate-well sorted sandstone.

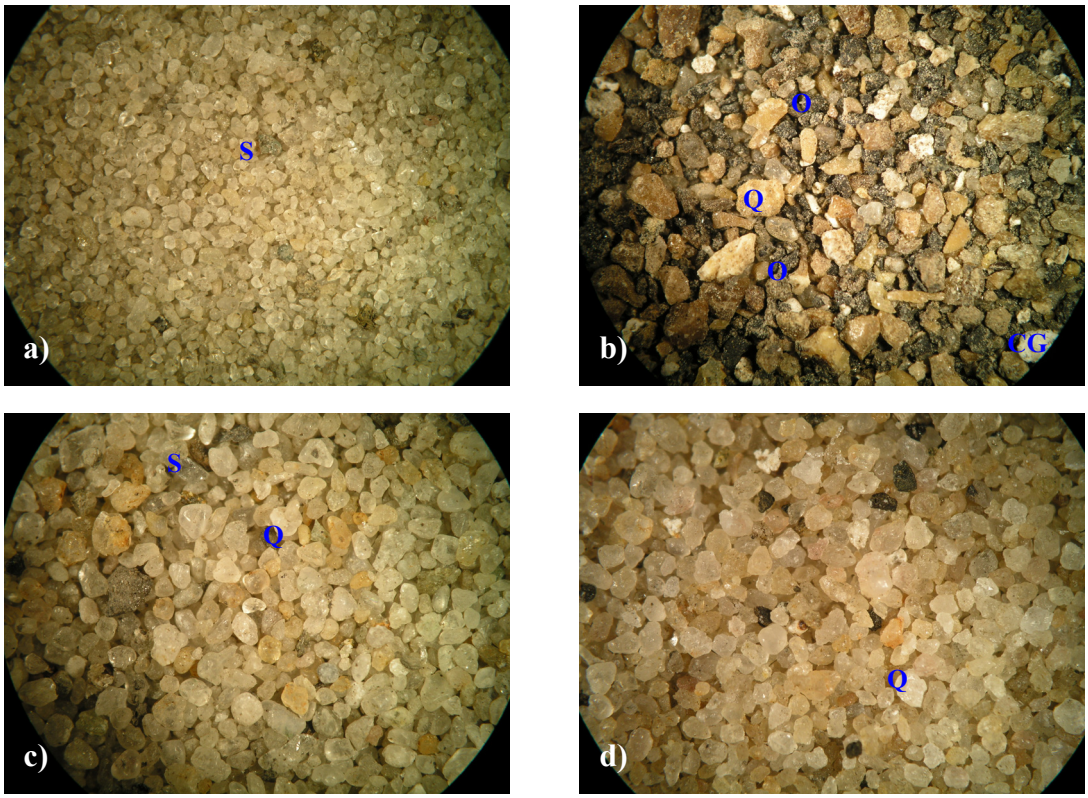

Figure 4. *Selected photomicrographs of siltstone/sandstone, sandstones and organic-rich material from Echuca Shoals-1. The field of view is approximately 14mm across. Key: S – shale fragment; CG – calcareous grain; Q – quartz; and O – organic material. a) Siltstone/sandstone with shale (1605-1610 m); b) Black, organic-rich material with quartz from just below the late Maastrichtian – Cenozoic boundary (1355-1360 m); c) Medium to occasionally coarse-grained Paleocene sandstone (1345-1350 m); d) Clean, well sorted Oligocene sandstone (940-945 m).*

Early Oligocene sandstone is clean, coarser grained, more angular with decreasing depth, and well-sorted before it begins to fine upwards and become poor-moderately sorted just beneath the transition to sandy carbonate grainstone found above 935 m RT.

Copernicus-1

Cenozoic sandstones are found in the Copernicus-1 well between 818 m and 1350 m RT. 19 samples were examined from the 54 samples that were collected every 10 m from this section of the well. The sediments in this section are Paleocene to Eocene in age and according to the well completion report, no Oligocene age sediments are present in the well.

The Paleocene is characterised by medium to very coarse-grained, sub-angular to rounded, poorly to moderately-sorted sandstone grading into calcareous and dolomitic sandstone with the same texture. This is overlain by Paleocene – Eocene fine- to coarsely-crystalline carbonate grainstone with occasionally up to 20% quartz grains.

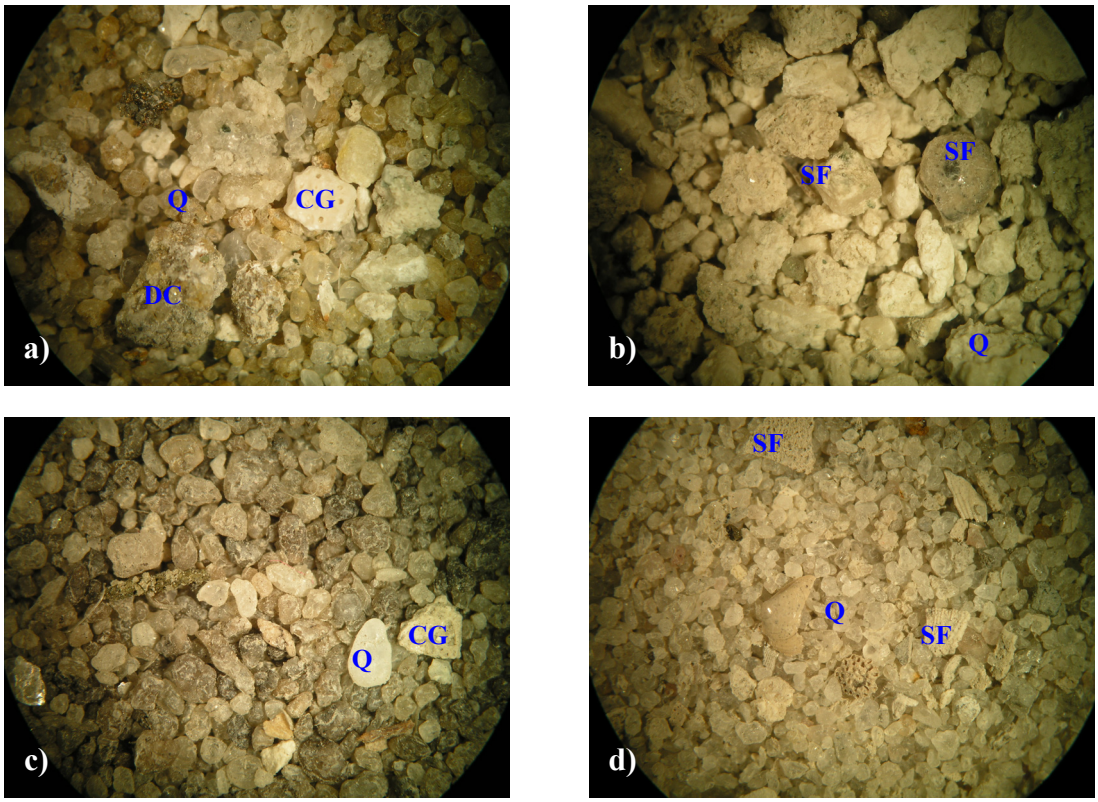

Figure 5: *Selected photomicrographs of sandstones and fossiliferous grainstone from Copernicus-1. The field of view is approximately 14mm across. Key: SF – skeletal fragment/fossil; CG – calcareous grain; Q – quartz; and DC – dolomite clast. a) Calcareous and dolomitic sandstone (1250-1260 m); b) Fine- to coarsely-crystalline carbonate grainstone (1210-1220 m); c) Muddy looking Eocene sandstone (1050-1060 m); and d) Medium to coarse-grained sandstone containing occasional skeletal fragments (850-860 m).*

In the Early Eocene section, the sandstone varies from fine to very coarse-grained throughout and is generally sub-angular to rounded and poorly-sorted, becoming well sorted in the top 20 m. It is also often coated with carbonate cement and is 'muddy' looking. Occasional shaly layers (~5% shale) are also present. The Middle Eocene interval is composed of a medium to coarse-grained, sub-angular to rounded, poorly to moderately sorted calcareous sandstone overlying an extremely fossiliferous grainstone. In the Late Eocene samples, medium to coarse-grained, sub-angular to rounded, moderately to well-sorted sandstone grades into calcareous sandstone (coarse-grained, sub-angular to rounded and poorly-sorted towards the top), before making the transition into calcareous packstone/grainstone. Selected photomicrographs of sandstones and fossiliferous grainstone from Copernicus-1 are shown in Figure 5.

Discorbis-1

Although samples were collected every 3 m from the Cenozoic sandstones present in the Discorbis-1 well, not all were available in Geoscience Australia's cuttings collection. Seventeen samples were examined from cuttings collected between 2046 and 2349 m; depending on which stratigraphic markers are used, the Cenozoic sands in Discorbis-1 fall either entirely within the Paleocene (BBHR) or span the Paleocene and Eocene. Selected photomicrographs of sandstones and fossiliferous grainstone from Discorbis-1 are shown in Figure 6.

The late Maastrichtian sediments at the base of the Cenozoic are composed of dolomitic, mainly coarse-grained and sub-rounded sandstone that also contains a significant proportion of sub-rounded to rounded, fine grains of quartz within dolomite fragments. Also present is an undetermined orange/brown mineral (Figure 6a and 6b) which could not be identified by XRD analysis.

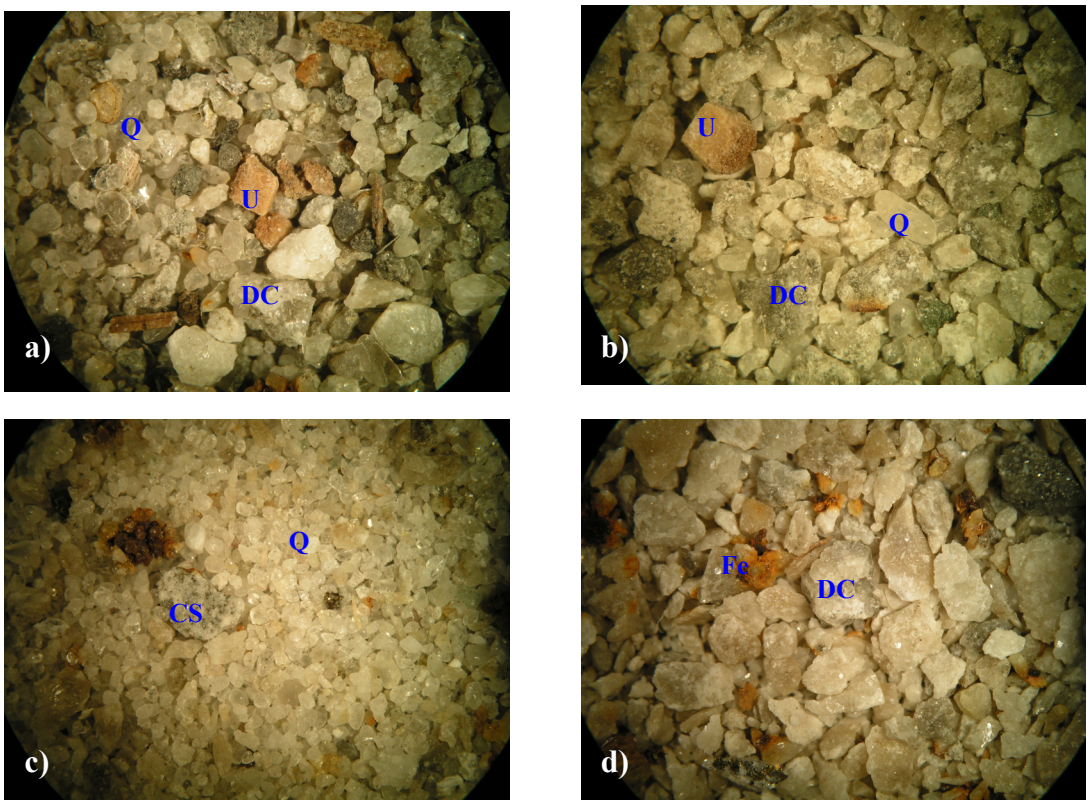

Figure 6: *Selected photomicrographs of sandstones and dolomite from Discorbis-1. The field of view is approximately 14mm across. Key: Q – quartz; DC – dolomite clast; U – unknown orange mineral; CS – calcareous silt and Fe – Iron staining/cementation. a) Unknown mineral in dolomitic sandstone (2349-2352 m RT); b) Dolomite unit with occasional rounded quartz grains (2229-2232 m RT); c) Dolomitic mid-Paleocene sandstone with occasional calcareous silt fragments (2109-2112 m RT); and d) Late Paleocene slightly sandy dolomite (850-860 m RT).*

The largest gap in cuttings in the Geoscience Australia sample set occurs over the Mesozoic – Cenozoic boundary. When cuttings resume in the Early Paleocene, they are of a 40 m thick layer of highly dolomitic sandstone (60%+ dolomite). In this unit several individual grains of quartz are very coarse grained but the majority of the quartz is actually fine grained and found within dolomite fragments.

Transitioning into dolomite with occasional, thick (30+ m), highly dolomitic sandstone interbeds, the quartz in this sequence fines upwards from coarse to medium-grained and also becomes more angular. In the mid-Paleocene the lithology reverts back to dolomitic, medium-grained, angular to sub-rounded, poorly to moderately sorted sandstone.

The Late Paleocene sees a change back to slightly sandy dolomite, with cuttings becoming less sandy with decreasing depth down-hole before changing again, this time to dolomitic, slightly sandy grainstone to packstone. The quartz present is coarse to very coarse-grained and sub-angular to sub-rounded.

Within Discorbis-1 the boundary between the Cenozoic carbonate sequences and the underlying Cenozoic sandstones is unclear as there were no returns over the shakers between 1580 m and 2046 m and it is within this interval that the change takes place.

Bassett-1a

Twenty seven cuttings samples were examined from the 164 samples collected every 5 m within the Cenozoic sandstone section of the Bassett-1a well. These Paleocene to Oligocene sandstones are often interbedded with dolomite, and can be found between 1120 m and 1940 m according to well completion reports. Selected photomicrographs are shown in Figure 7.

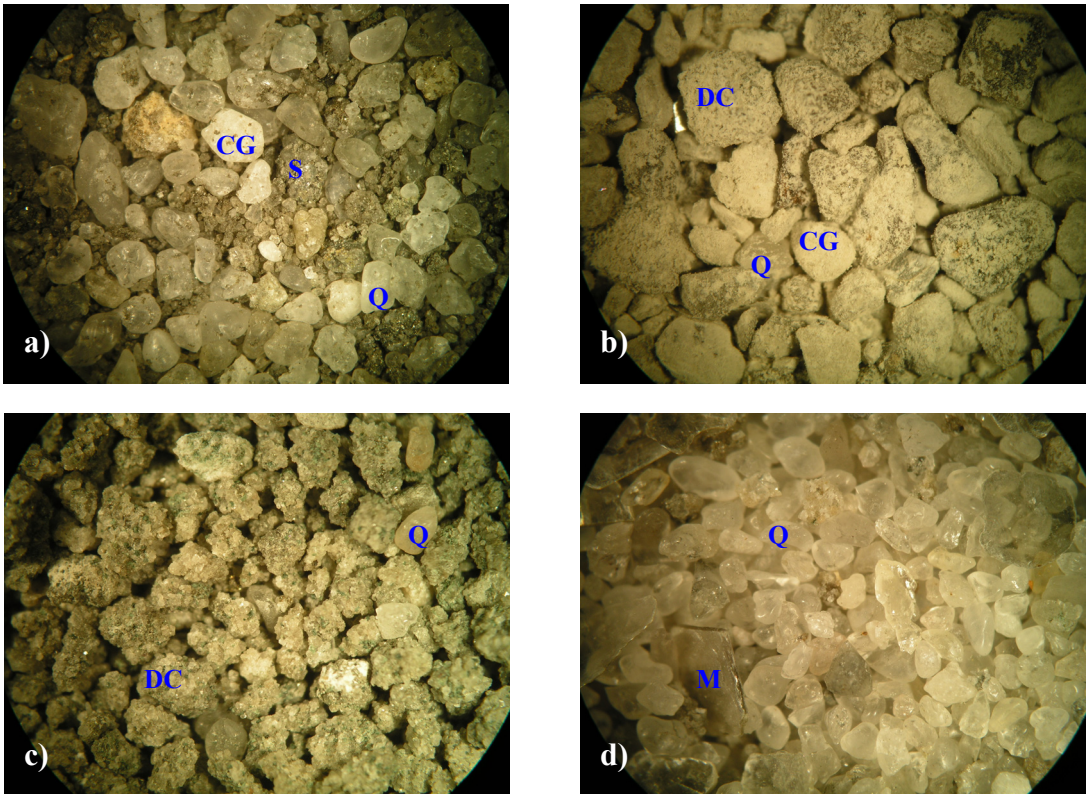

Figure 7: *Selected photomicrographs of shaly siltstone, sandstones and dolomite from Bassett-1A. The field of view is approximately 14mm across. Key: Q – quartz; DC – dolomite clast; CG – calcite grain; M – Mica; and S – Shale/silt. a) Silty early Cenozoic sandstone with shale (1700-1705 m); b) Dolomitic sandy packstone at the Eocene – Paleocene boundary (1475-1480 m); c) Coarsely crystalline Early Oligocene dolomite containing fine quartz silt - greenish colour caused by glauconite (1455-1460 m);d) Mid-Oligocene sandstone with drilling mud mica (1310-1315 m).*

The late Maastrichtian interval in Bassett-1a is composed of silt to granule sized, moderately to poorly sorted, silty sandstone with grains of varying angularity. This changes to a very fine to very coarse-grained, dolomitic, silty sandstone, which increases in angularity and becomes better sorted with decreasing depth. A thin (approx. 15 m thick) sandstone layer lies above the dolomitic silty sandstone and is in turn overlain by approximately 100 m of dolomitic, silt/very fine to granule-sized, sub-angular to sub-rounded sandstone, that changes from moderately sorted to poorly sorted with decreasing depth. Some shale is found towards the top of the section, at the base of the Cenozoic.

The Early Paleocene is composed of dolomitic sandstone, with coarse to granule-sized, angular to sub-rounded and poorly sorted grains, that becomes very fine to very coarse, angular to rounded and very poorly sorted sandstone in the Middle to Late-Paleocene.

Early Eocene sediments are dolomitic, coarse to very coarse, angular to rounded and poorly sorted sandstone overlain by dolomite containing fine quartz silt. The Eocene – Oligocene boundary is marked by a calcareous dolomitic sandy packstone, which is overlain by another interval of dolomite containing fine quartz silt. Above this unit is a highly dolomitic medium to coarse-grained, angular to rounded, poorly sorted sandstone with a dolomitic sandy packstone at its base.

Occasionally calcareous sandstone that is very coarse to medium grained and poorly to moderately sorted with decreasing depth overlies the dolomitic sandstone; grain shape varies from sub-angular to rounded. The Late Oligocene sediments then transition from sandstone into sandy packstone into grainstone over packstone.

Caswell-2

Cuttings were collected every 5 m from Paleocene to Eocene aged sandstones present between 1730 m and 2595 m in the Caswell 2 well, and 20 samples were selected from a possible 173 for closer examination. Examples of the lithology described in this section are shown in Figure 8.

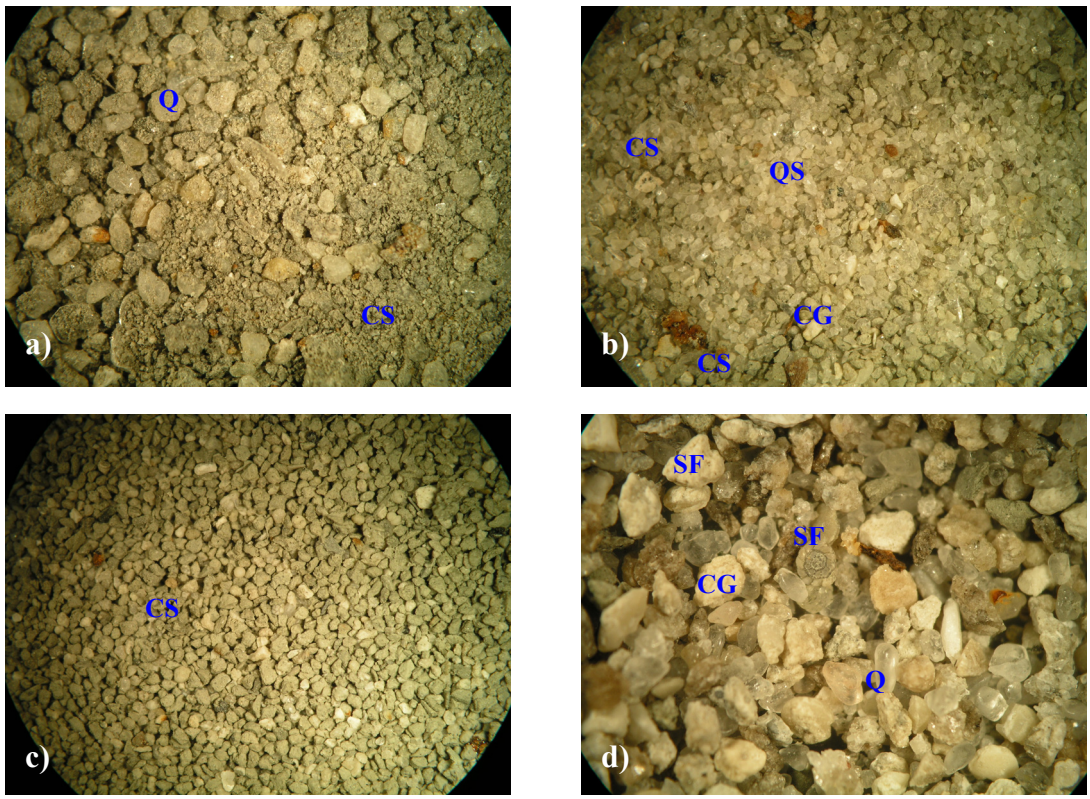

Figure 8: *Selected photomicrographs of shaly siltstone, sandstones and dolomite from Caswell-2. The field of view is approximately 14mm across. Key: Q – quartz; QS – quartz silt; CG – calcite grain; CS – calcareous silt; SF – skeletal fragment/fossil and S – Shale/silt. a) Base Paleocene calcareous silt/sandstones (2595-2600 m); b) Middle Paleocene calcareous silt/sandstone (2355-2360 m); c) Thin Middle Eocene wackestone layer (1995-2000 m); and d) Middle to Late Oligocene, calcareous sandstone containing skeletal fragments (1750-1755 m).*

At the base of the Paleocene in Caswell-2 are calcareous silt/sandstones that contain quartz silt in addition to the calcareous silt seen elsewhere in the well. Above these lies an approximately 50 m thick shaly/claystone layer, in turn overlain by a calcareous, medium-grained, angular to sub-rounded, well to moderately sorted silty sandstone unit that contains occasional medium/coarse, sub-angular to sub-rounded, well to moderately sorted sandstone layers.

The Middle Paleocene is comprised of more calcareous silt/sandstone (30% calcareous silt), that is fine to medium-grained, angular to sub-angular and well to moderately sorted. This unit is overlain by well to moderately sorted calcareous sandstone that is fine to coarse-grained and increases in grain angularity with decreasing depth.

The Eocene is represented by an approximately 50 m thick unit of sandy packstone/grainstone that contains skeletal fragments (unlike the upper part of this sequence) overlain by calcareous sandstone containing occasional thin wackestone layers. This sandstone varies from medium to very coarse-grained, is poorly sorted (occasionally well sorted) and grains are angular to sub-angular.

Sandstone in the Oligocene has medium to granule-sized grains that are sub-angular to rounded and are moderately sorted, and is calcareous, containing skeletal fragments and up to 10% calcareous silt.

X-RAY DIFFRACTION (XRD) ANALYSIS

5 cuttings samples were sent for XRD analysis: Caswell-2 1950 m; Discorbis-1 2046 m; Discorbis-1 2349 m; Echuca Shoals-1 1355 m; and Echuca Shoals-1 1365 m. The analytical results are presented in Appendix 7.

The two Echuca Shoals-1 samples were analysed to aid identification of an unknown orange mineral present in the organic-rich cuttings samples and in selected samples from Discorbis-1. This mineral proved extremely difficult to crush and could not be analysed. The remainder of the samples were determined to be predominantly quartz with some calcite, gypsum and micas. The analysis of a sample of the Discorbis-1 2046 m cuttings determined that the rusty coloured iron mineral present was ankerite.

FACIES ANALYSIS AND DESCRIPTION OF WIRELINE LOG RESPONSE

Gamma ray and sonic logs, density neutron suite and spontaneous potential logs were run in the five wells under investigation. In this study particular attention was given to the gamma ray and sonic logs. A diagram displaying the wireline logs, BBHR derived seismic markers and lithological summaries for each of the five wells can be found in Appendix 5. As discussed in earlier there is a discrepancy between the BBHR seismic marker for the base of the Cenozoic and the marker assigned to the same boundary within the well completion reports for three of the five wells that have been examined. In the following discussion of wireline log response the BBHR marker has been used as the base Cenozoic marker, with the response below this marker being described as being late Maastrichtian in age. The typical sandstone gamma ray ‘baseline’ response seen in the wells is 5 – 10 API.

Wireline logs can give good indication of lithology, and therefore palaeoenvironment; however, there are many instances in this comparison of logs to observed lithology where there appear to be discrepancies. One probable explanation for this is that due to the drilling and processing method, the cuttings that were examined are not necessarily the best representation of actual lithology.

Echuca Shoals-1

Within the late Maastrichtian the gamma ray response is highly variable with numerous 55 to 75+ API peaks that correlate well with the observed lithology of the cuttings, corresponding to siltstone layers and the two organic rich layers. A 75 API peak marks the BBHR base Cenozoic marker before the response gradually drops to 10–15 API (over 30 m).

Throughout the Cenozoic the gamma ray log response for Echuca Shoals-1 remains very low and very stable, displaying a 'baseline' of 5-15 API that is repeated in each of the other 4 wells for which the wireline logs were examined. Two small peaks (25 and 30 API respectively) are seen just below the Paleocene – Eocene boundary and in the Middle Eocene. The transition from sandstone to carbonate deposition in the Middle Eocene is not marked by a change in the gamma ray response.

In contrast to the gamma ray log, the sonic log can be quite variable. In general Echuca Shoals-1 has produced a higher sonic response throughout than any of the other wells examined. Within the late Maastrichtian, the log response is relatively stable with one prominent drop in response coinciding with a siltstone layer, most likely indicating a drop in porosity. However, there is a general trend implying increasing porosity with decreasing depth reaching a maximum near the late Maastrichtian – Paleocene boundary. In the Early Paleocene the response decreases again. The Middle Paleocene exhibits a fairly stable response interrupted between 1255 m and 1295 m by a highly fluctuating response.

Although oscillating, in the Late Paleocene the response begins to increase and continues to do so through the Paleocene – Eocene boundary and throughout the Eocene, indicating a slight increase in porosity up-hole. The sandstone-carbonate transition is marked by a slight decrease.

Copernicus-1

In Copernicus-1 a sharp spike in the gamma ray response to 75+ API marks the base of the Paleocene, while the Early to Middle Paleocene has a stable but slightly elevated response (15 – 30 API) compared to the typical sandstone 'baseline' response (5 – 10 API) seen in the other four wells. In the Middle Paleocene the baseline response drops slightly coinciding with a change in lithology from calcareous dolomitic sandstone to grainstone. This response continues throughout the Eocene, with no change in the log at the Paleocene – Eocene boundary. Only two spikes interrupt the continuity of the log. The first is a 50 API peak over 30 m at around 1100 m, towards the base of a sandstone unit that contains occasional shaly layers. The second peak is smaller (~35 API), and occurs within a fossiliferous grainstone unit. There is no sonic log for Copernicus-1.

Discorbis-1

The late Maastrichtian to Paleocene is represented in the gamma ray log by repeated high amplitude spikes (75+ API), which corresponds to the well completion report description of sandstone interbedded with argillaceous sandstone and claystone. The sonic log for this section is stable, ranging from 80 – 100 us/ft.

Just below the BBHR base Cenozoic marker the sonic log begins to increase in amplitude and oscillate, and this response continues into the Lower Paleocene. Over the same interval the gamma ray drops to 10 – 15 API (baseline) but contains two slightly graduated peaks (55 API and 45 API respectively). One peak marks the boundary between a section of the well with no samples (that covers the base of the Cenozoic), the other a change from dolomitic sandstone to dolomite.

The gamma ray response throughout the remainder of the Paleocene is low except for a wide, graduated peak in the Late Paleocene that correlates with a dolomitic packstone layer. The sonic

response is more variable over the rest of the Paleocene, sharply decreasing twice in the Middle Paleocene and then oscillating over a range of 30 us/ft but steadily increasing from 50 – 80 us/ft to a 100 – 130 us/ft. The drops in sonic response correspond well with the dolomite lithology of this section of the well, while the increases match sandier layers within the dolomite. A significant spike in the sonic log occurs at 2100 m, the boundary between a dolomitic sandstone unit and the sandy dolomite unit above it. A significant drop in the sonic log within this sandy dolomite unit also corresponds to a low sand/high dolomite section implying a lower porosity/higher degree of cementation.

There were no returns over the shakers within the Discorbis-1 well between 1580 m and 2046 m. This interval corresponds to the location of the transition from sandstone to carbonate in this area of the basin. No sonic response was recorded above 2046 m and the gamma ray response gives no real indication of a possible boundary, remaining between 5 and 20 API throughout the section.

Bassett-1A

During the late Maastrichtian to Paleocene frequent large (55 – 75+ API) gamma ray spikes are recorded. A notably large spike at 1820-1840 m corresponds to a lithological change from dolomitic silty sandstone to sandstone. This change is also marked by a decrease in the sonic log, possibly indicating a decrease in porosity. A slight increase in the sonic log just below the BBHR recognised base of the Cenozoic, and a small peak in the gamma ray (~40 PI), mark the boundary.

The gamma ray response is baseline throughout the Paleocene and Eocene while during the Early to Middle Paleocene the sonic log is low (60 – 100 us/ft) with a relatively frequent oscillation. The sonic log stabilises before again increasing in oscillation in the Late Eocene. No changes in either of the logs appear to indicate significant changes in the lithology of the well; however the Paleocene to Eocene boundary is marked by an increase in the gamma ray (over 50 m) to 45 API, and a corresponding drop in the sonic log. Both of the logs support the observed lithology of a dolomitic sandy packstone, which is expected to have a smaller grain size and lower porosity than the units above and below.

The Oligocene interval displays a response similar to that seen in the Eocene units before dropping sharply again within a highly dolomitic sandstone, perhaps reflecting a high level of cementation. Apart from a 50 m gap in the sonic log, the signal remains higher for the rest of the Oligocene. A short, sharp drop in the sonic log may reflect the change from sandstone to packstone at ~1180 m. There is no corresponding change in the gamma ray log.

The Early to mid-Oligocene gamma ray log is variable with a series of 30 – 50 API spikes followed by base level readings.

Caswell-2

The basal 50 m of shale in Caswell-2 is represented on the wireline logs by a fluctuating increase in the gamma ray response (from baseline to 60 API) that indicates the presence of clays/fine material. The remainder of the Paleocene has a low gamma ray response with two significant broad peaks of ~40 API that correspond with a calcareous silt-rich layer and a calcite rich layer respectively. The sonic log remains stable at with a ~40 m section of highly variable response that corresponds to a layer of clean sandstone.

The Paleocene – Eocene boundary is marked by a decline in the sonic log response which subsequently becomes more constant with decreasing depth and, just above the boundary, a small spike in the gamma ray response. Although the sandstone in Caswell-2 is very often calcareous, this

change in the logs marks the first real carbonate layer to be seen in the Cenozoic. The gamma ray log throughout the Eocene remains at baseline with a small spike in the log correlating with a thin calcareous siltstone layer.

The Eocene – Oligocene boundary is again marked by a change in the sonic log, which becomes highly oscillating, remaining so for the entire Oligocene interval. A jump in oscillation range (to 55-140+ us/ft) corresponds to the change in lithology from calcareous sandstone to sandy pack/grainstone.

The gamma ray log remains low with two small spikes (45 API) that correlate well with two silty sandstone layers. No change in gamma ray response is observed at the sandstone-carbonate boundary.

PALAEOENVIRONMENTAL INTERPRETATION

Based on the information in well completion reports, cuttings descriptions and wireline logs, an attempt has been made to identify the depositional environments over time for each well.

Echuca Shoals-1

In the late Maastrichtian, sandstone overlain by organic-rich material implies a fluvio-deltaic to lagoonal environment. This was overlain by clean coarse sandstone in the Paleocene, indicating a shift from a lagoonal to a fluvio-deltaic environment. This theory is supported by the decrease in the gamma ray response. The gamma ray log then suggests a steady state aggradational environment. Cuttings composed of sandstone indicate a continued fluvio-deltaic environment into the Eocene and Oligocene. The change to carbonate grainstone in the Late Oligocene represents a change to a deeper water, inner to mid-shelf environment.

These determinations support the conclusions made in Stephenson and Cadman (1994). They interpreted a fluvio-deltaic to lagoonal environment in the Paleocene and inner-shelf to marginal marine conditions in the Eocene – Oligocene, although no carbonate was found any of the Echuca Shoals-1 sandstones (which might be expected if they were deposited in a marginal marine environment).

Copernicus-1

As described earlier, the lithology of Copernicus-1 alternates between sandstone and carbonate sequences throughout the Paleocene and Eocene. Sandstone and dolomitic sandstone observed in the Paleocene interval, combined with a stable gamma ray response, indicates an aggradational fluvio-deltaic environment. A transition to grainstone, together with a corresponding slight drop in the gamma ray log, suggests inner- to mid-shelf conditions. The carbonate cement and ‘muddy’ appearance of this sandstone imply continued inner- to mid-shelf deposition. There is a return to sandstone deposition in the Early Eocene. The lack of carbonate material within this sandstone implies a return to fluvio-deltaic conditions or reworking of the sands prior to burial by a ~40 m thick layer of highly fossiliferous grainstone. The grainstone layer probably indicates the development of a reef system, although a seismic line (BBHR 12), running from inner- to outer-shelf through two nearby wells with an otherwise similar lithology to Copernicus-1 (Productus-1 and Asterias-1), shows no evidence of significant reef development implying that any reef development may have been quite localised.

Sandstones and a stable gamma ray log response are found above this grainstone layer, implying continued fluvio-deltaic conditions transitioning into marginal marine with a change to calcareous sandstone and then grainstone with increasing water depth.

Discorbis-1

Deposition of sandstones and dolomitic sandstones in the Paleocene, coupled with a fairly stable gamma ray response, are indicative of fluvio-deltaic to marginal marine conditions. As discussed in the section on wireline log response, peaks within the wireline logs are most likely related to cementation changes within the section. An increase in the gamma ray response in the Late Paleocene coincides with a dolomitic pack/grainstone unit and possibly indicates a transition to an inner to mid-shelf environment.

This interpretation is slightly different to the Paleocene palaeoenvironment indicated by Stephenson and Cadman (1994). Although their research did not incorporate data from Discorbis-1, superimposition of the well on to their Paleocene time-slice map indicates a mid-shelf to sandy inner-shelf environment.

Bassett-1a

A highly fluctuating gamma ray response and highly variable lithological texture in the late Maastrichtian sandstones indicate an inner-shelf to marginal marine environment, although the absence of carbonate material may indicate re-working.

Paleocene sandstones exhibiting a generally fining upwards grain size signify a stable marginal marine to inner-shelf aggradational environment that remains a fairly stable, aggrading environment, as represented by a steady gamma ray log.

The gamma ray response remains relatively stable throughout the Eocene where dolomitic sandstone is overlain by dolomite containing fine quartz silt indicating lower energy conditions in a probable inner shelf environment. A thin calcareous packstone layer overlain by another unit of dolomite containing fine quartz indicates a fluctuation between mid and inner-shelf conditions from the Late Eocene into the Early Oligocene.

Another thin layer of packstone in the Early Oligocene overlain by dolomitic sandstones again indicates a mid to inner-shelf environment. In the Middle Oligocene occasionally calcareous sandstone is suggestive of sandy inner-shelf conditions, before the transition to a mid to outer-shelf environment as indicated by the deposition of sandy packstone and grainstone.

These deductions are consistent with the Paleocene prograding inner sandy shelf and Eocene – Oligocene mid-shelf conditions proposed by Stephenson and Cadman (1994). They also support the palynological evidence within the well completion report for Bassett-1a that concludes a near shore environment in the Paleocene.

Caswell-2

The calcareous nature of the sandstones in the Early Paleocene and the presence of a shaly layer, combined with a series of large peaks in the gamma response for Caswell-2, point to either a fluvio-deltaic to marginal marine or near shore/lagoonal palaeoenvironment. The subsequent thick sequence of calcareous sandstone and low, stable gamma ray characterised by 2 broad peaks correlating with a calcareous silt-rich layer and a calcite rich layer respectively, are suggestive of mid to inner-shelf conditions.

The Eocene sandy packstone containing skeletal fragment and associated gamma ray peak indicate a mid-shelf environment of deposition. The return to a calcareous siltstone/sandstone in the Late Eocene and occasionally silty, calcareous sandstone throughout the Oligocene, matched by a stable gamma ray response with peaks that relate to silt-rich layers, indicates an aggrading, mid to outer-

shelf environment. Again these observations support the palaeoenvironment conclusions of Stephenson and Cadman (1994).

STRATIGRAPHIC BOUNDARIES

When collating the wireline log responses, seismic horizon information and cuttings lithology of the five wells differences were noted in the allocation of the base Cenozoic marker within three wells, Echuca Shoals-1, Discorbis-1 and Bassett-1a.

Echuca Shoals-1

In Echuca Shoals-1 the BBHR seismic survey placed the base Cenozoic marker (Tbase) at a depth of 1353 m, compared to the 1512 m depth indicated by the well completion report; a difference of 159 m. Examination of the wireline logs shows that the gamma ray log above the BBHR Tbase boundary is constant (between 7-15 API) while below the boundary there are several sharp spikes (from 15 up to 75 API) indicating a differing lithology. As discussed earlier, a change in lithology was seen during the cuttings examination, which showed two organic material-rich samples separated by a clean sand layer just below Tbase.

The well completion report states that there were no foraminifera present with which to date the Mesozoic – Cenozoic boundary and that a depth of 1512 m was tentatively picked on the basis of seismic and electronic log correlation. However the BBHR seismic profile (BBHR 10) shows clear onlaps and downlaps above and below BBHR Tbase marker. This evidence combined with the gamma ray log response, supports the position of the BBHR Tbase marker at 1353 m RT.

Discorbis-1

In Discorbis-1 the Tbase depth of 2554 m suggested in the well completion report was contradicted by the allocation of the BBHR base Cenozoic marker to 2311.8 m RT; a difference of 242.2 m. Like Echuca Shoals-1, the units around the Mesozoic – Cenozoic boundary in Discorbis-1 are barren of biostratigraphic indicators, so the determination of the boundary found in the well completion report was “made with great uncertainty due to age dating problems” (Discorbis-1 Well Completion Report, BHP Petroleum, 1989).

As in Echuca Shoals-1, the gamma ray log for Discorbis-1 shows a significant change in response from low and consistent above the BBHR Tbase marker to a series of large (45 to 75+ API) peaks, while clear onlaps and downlaps above and below the Tbase marker on the BBHR Seismic profile (BBHR 15) also support its position at 2311.8 m.

The well completion report for Discorbis-1 also interprets differing depths for the base of the Paleocene (2238 m versus 2020 m) and the base of the Eocene (1452.5 m versus 1994 m). The Paleocene – Eocene boundary in particular seems highly unlikely when compared to the BBHR seismic markers; at 1452.5 m the BBHR has interpreted the Early – Middle Miocene boundary.

Bassett-1a

In Bassett-1a Cenozoic sandstones can be found between 1120 m and 1940 m, according to well completion reports. However, differences exist between the reports and the BBHR seismic survey, which puts Tbase at 1714 m RT, a difference between the two of 229 m.

The well completion report puts the base of the Cenozoic at 1943 m for a number of reasons. Although the section 1862 – 2023 m was indeterminate (because it is barren), Tbase was placed on the basis of a log break (Woodside Petroleum, 1978). Additionally, the absence of palynological evidence (Senonian [Turonian to Maastrichtian] microplankton) between 1862 m and 1906.5 m was

taken to be negative evidence. The highest occurrences of *Dinogymnium acuminatum* and *Dinogymnium westralium* are at 1943.5 m and these are interpreted to be evidence for the top of the Maastrichtian.

Although there is a ~45 API peak in the gamma ray response at the BBHR Tbase (Base Cenozoic) marker, the response does not begin to show the series of large peaks seen in both Echuca Shoals-1 and Discorbis-1, and the other two wells examined closely, until a depth of ~1800 – 1830 m. As described earlier the sonic response also decreases at this depth. Together these logs suggest that the BBHR marker may be too shallow. Evaluation of the BBHR seismic profile (BBHR 11 and BBHR 15) also indicates that the seismic evidence for the current BBHR Tbase marker is less conclusive than in Echuca Shoals-1 and Discorbis-1. Therefore evidence exists to support a lower base Cenozoic marker, although not at the depth specified in the well completion report.

POROSITY AND PERMEABILITY

Important factors in the suitability of a sandstone sequence for CO_2 storage are the porosity and permeability characteristics of the unit. If the sandstone is not porous then it will have a very small storage capacity and if it is not permeable then injected CO_2 will not be able to migrate into the unit. Good porosity for CO_2 storage is between 10 and 50% (Bradshaw and Bradshaw, 2000).

The porosity data that was available within well completion reports has been summarised (Appendix A6). Most often, reported porosity was based upon a visual estimation of samples rather than log data and the basis on which the porosity determination was made is not clear. As no independent and systematic approach to porosity determination was used the available porosity data is subjective indicating a need to be cautious when making comparisons between wells.

This caveat not withstanding, the visually estimated porosity within sandstone units from wells across the Browse Basin is generally fair to very good. Within individual wells a range of porosities is usually evident reflecting the varying lithology. For example, porosity is often reduced within highly calcareous or silty units. Log porosities are usually given as relatively large ranges (e.g. 8 – 37% in Caswell-2); this is most likely caused by heterogeneity and interbedding within individual sequences.

Permeability data was rarely available in any of the available well completion reports. However the GEODISC report (Bradshaw and Bradshaw, 2000) refers to low permeability in the Browse Basin sandstones, which may present problems for CO_2 injection at sub-surface depths >2700 m. However the Cenozoic section is reported as having good porosity and permeability (Bradshaw and Bradshaw, 2000); the bases of all the Cenozoic sandstone units investigated lie above 2700 m.

Due to the nature of drilling, the sandstone cuttings that were examined did not provide suitable samples for porosity and permeability testing. MICP testing requires samples that are no less than 4mm thick. Although fragments larger than 4 mm do exist within the cuttings record, there were usually clear indications that this texture was post drilling and that the clasts were actually created by clumping together of wet grains, often cemented by drilling mud.

RESERVOIR WITH THE HIGHEST POTENTIAL FOR CO_2 STORAGE IN THE CENOZOIC SANDSTONE SECTION OF THE CASWELL SUB-BASIN

Another factor critical to any investigation of the suitability of a sandstone sequence to provide a reservoir for CO_2 storage is the depth of the top of the reservoir. In order to maintain the supercritical state of the CO_2, it must remain below a depth of 800 m below sea level.

Mapping the depth within each well to the top of the Cenozoic sandstones (Figure 9) illustrates that wells along the south-eastern (continental) margin of the Browse Basin encountered Cenozoic sandstones at depths above 800m below sea level. Therefore this section of the basin is considered unsuitable for CO_2 storage.

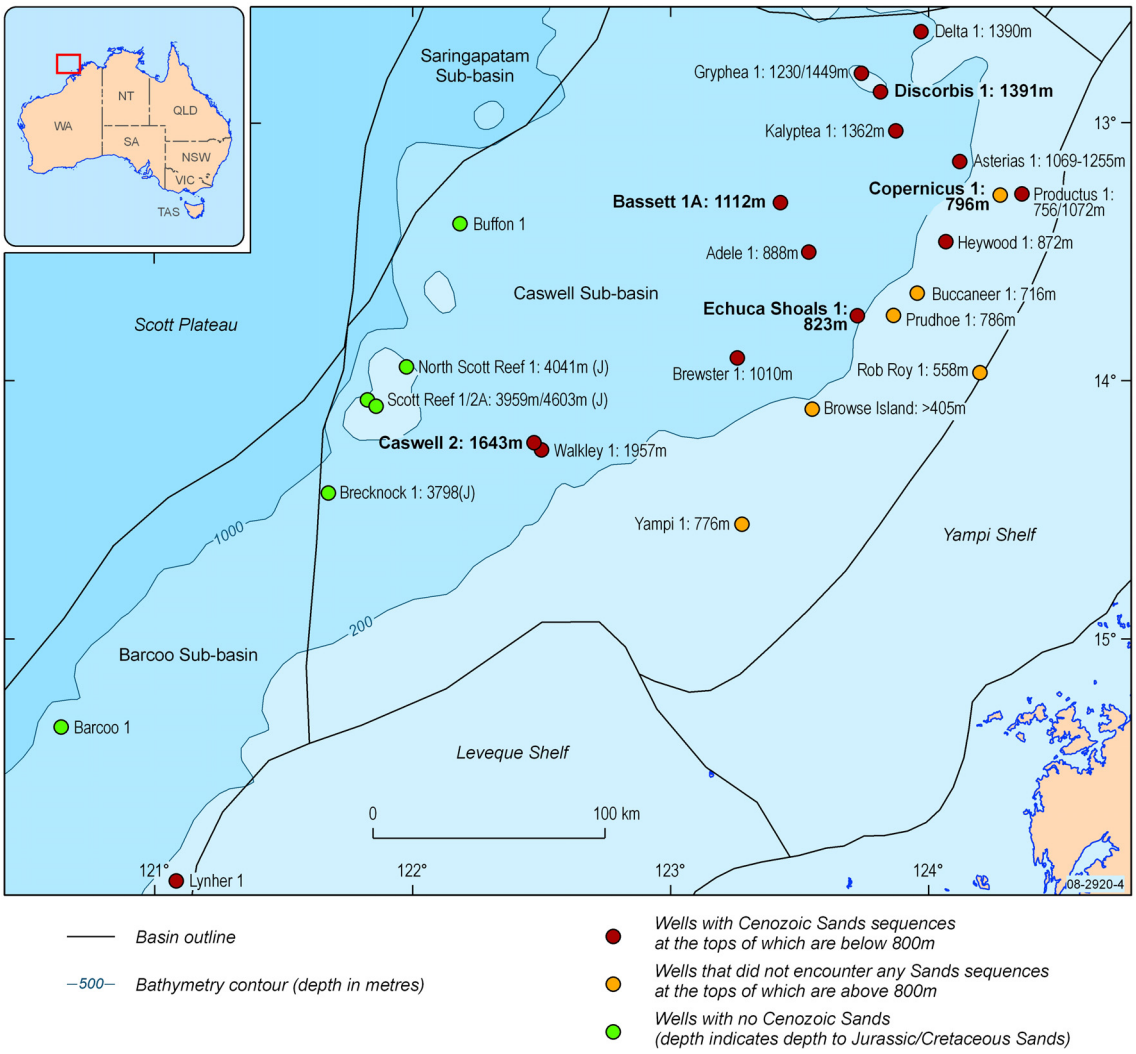

Figure 9: *Depth to the top of Cenozoic sandstones in wells in the Barcoo and Caswell Sub-basins.*

Taking all of the information presented in this section into consideration, the best potential CO_2 reservoir in the central Browse Basin is within the central Caswell Sub-basin around the Caswell-2 well site. The sandstone sequence in this area of the basin is thick and laterally extensive with good porosity and permeability and is situated well below supercritical depth. This stratigraphic section is also not currently an exploration target in the basin (Bradshaw and Bradshaw, 2000) so the risk of hydrocarbon field contamination by CO_2 is low.

This conclusion supports findings of Bradshaw and Bradshaw (2000), who also considered the Cenozoic age sandstones within the Browse Basin to have the highest potential for successful CO_2 injection, dependant on the ability of the thick overlying carbonate sequences to provide an adequate seal.

A further consideration is the structural integrity of any potential reservoir and this information will be discussed later in the seismic interpretation section of this report.

Cenozoic Carbonates

INTRODUCTION

The collection, description, analysis, and ultimately the interpretation of the Cenozoic carbonate section of the Browse Basin has been limited as this sequence appears to have been of minimal interest to those exploring for oil and gas. Nonetheless, the distribution, lithological character, palaeogeographic deposition and ultimately the potential sealing capacity of the carbonate sequence has been determined using well completion reports, analysis of the cuttings held at Geoscience Australia and changes in wireline-log response.

CENOZOIC CARBONATE DISTRIBUTION WITHIN THE BROWSE BASIN

The review of the well-completion reports has revealed significant variability in the Cenozoic carbonate thickness in the Browse Basin (Figure 10). Most striking are the considerable carbonate thicknesses - that are assume to continue up to the current seafloor - in the north-western Caswell Sub-basin and in the central Barcoo Sub-basin, ranging from ~2000 to 3500 m. Coincident with these thick carbonate sequences is an absent lower sandstone layer (Figure 10). Thus, as these regions do not have the requisite reservoir for CO_2 storage they are not discussed further in this report.

The thickest carbonate sequence that is also associated with a significant Cenozoic sandstone reservoir is located in the central Caswell Sub-basin. Here the Caswell-2 and Walkley-1 wells penetrate ~1300 to ~1600 m of carbonates which are underlain by ~500 to 1000 m of Cenozoic sandstone. The central Caswell Sub-basin near Bassett-1a and Brewster-1 also has a substantial carbonate thickness of ~600 to ~700 m, and ~600 to ~1100 m of underlying Cenozoic sandstone. In the eastern and northern portions of the Caswell Sub-basin the carbonates and sandstones do not have the dichotomous relationship that is seen elsewhere in the basin. Instead, relatively thin sandstone and carbonate units are intercalated throughout the Cenozoic, with a change from dominantly clastic deposition early in the Cenozoic to mostly carbonate deposition later in the Cenozoic.

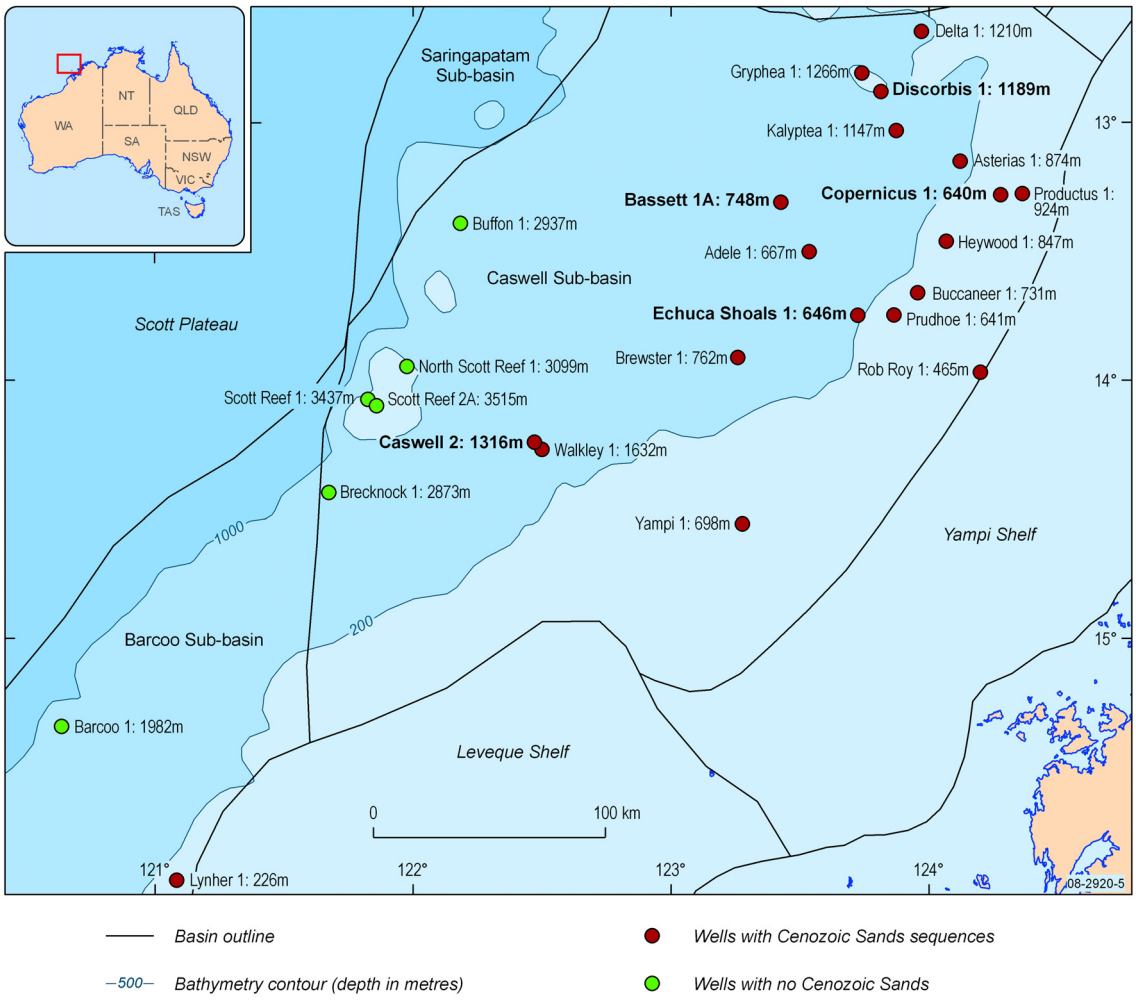

Figure 10: *Thickness of the Cenozoic carbonate sequence in each well with the assumption that the carbonates continue to the current seafloor. The location of the wells within the Browse Basin are differentiated into two categories, those that contain Cenozoic Sandstone (in red) and those that do not contain Cenozoic sandstone (in green)*

CARBONATE LITHOLOGIES AND INFERRED ENVIRONMENTS OF DEPOSITION

Cuttings from the Cenozoic carbonate sections at Discorbis-1, Copernicus-ST1, Bassett-1a, Echuca Shoals-1 and Caswell-2 were examined to constrain carbonate sequence stratigraphy, seal capacity and palaeogeographic environment. The process of selection resulting in these wells was discussed in an earlier section.

A general description of the carbonate lithologies in each well is provided below with individual detailed cutting descriptions provided in Appendix 2. However, it is important here to make a brief comment about the degree of consolidation observed in the carbonate cuttings. The cuttings range from completely unconsolidated (majority) to consolidated. Samples with high proportions of clay or mud are often moderately consolidated whereas samples with minimal clay or mud or a high fossil content are typically unconsolidated. A significant consolidated carbonate section was observed in Bassett-1a where very hard chips up to 6 mm in size were observed.

Description and Classification Terminology

The terminology used to describe the cuttings in the following discussion and Appendix 2 includes: the Udden & Wentworth grain size scale (Wentworth, 1922); the Compton (1962) sorting classification; and grain shape based on the AMSTRAT (American/Canadian Stratigraphic) size-class comparison classes. The approximate proportion of calcite grains, calcareous clay/silt (micrite), skeletal fragments, quartz and accessory phases were estimated using the following guidelines: 1 - calcite grain includes calcite aggregates in which the individual crystals are greater than 30 μm; 2 - finely crystalline calcite describes crystal sizes from 30 μm to 1 mm; and 3 - coarsely crystalline describes crystals >1 mm. The calcareous clay/silt is typically observed as clasts of microcrystalline calcite that range up to 1 cm in size. As the individual grain size and texture was not determined, the calcareous clay/silt is recorded as representing micrite (microcrystalline calcite). For the purposes of this report the micrite is assumed to represent a combination of calcareous mud and/or post-depositional cementation. Finally, "skeletal fragment" is an inclusive term for any fossil or biological material visible under the binocular microscope.

The carbonate classification follows a slightly modified version of Dunham (1962) as Dunham's original classification required thin-section analysis, a methodology not feasible with the well cuttings available for this study. Consequently, Dunham's classification has been adapted to enable broad carbonate classification using a binocular microscope (Table 1).

Table 1: The original Dunham (1962) and the modified Dunham classification used in this report.

CARBONATE CLASSIFICATION	ORIGINAL DUNHAM CLASSIFICATION	MODIFIED DUNHAM CLASSIFICATION USED IN THIS REPORT
Mudstone	Mud supported with less than 10% coarser grains	Sample contains more than 90% calcareous clay/silt
Wackestone	Mud supported with more than 10% coarser grains	Sample contains between 50 and 90% calcareous clay/silt and more than 10% coarser grains
Packstone	Grain supported but with a sparse muddy matrix	Sample contains more than 10% and up to 50% calcareous clay/silt, and is thus grain supported with a sparse muddy matrix
Grainstone	Grain supported and with no muddy matrix.	Sample does not contain calcareous clay/silt and is instead composed of skeletal fragments and calcite grains.

Echuca Shoals-1

Eleven samples were selected from the carbonate section of Echuca Shoals-1 and range from 530 to 920 m depth. Generally the samples are free of calcareous clay/silt, with more than 50% calcareous clay/silt only observed in three cuttings, the first below the inferred Oligocene lowstand and subsequently in two samples near the top of the section (Figure 11). Skeletal fragments were found in all cuttings, and ranged from 10 to 50% in abundance. Quartz grains and an iron rich mineral inferred to be ankerite or siderite were found throughout most of the section. Selected photomicrographs of Echuca Shoals-1 carbonates are shown in Figure 11.

The lower portion of the carbonate section appears to have been deposited as water depth in the basin increased. Finely to coarsely crystalline calcite is replaced by calcareous clay/silt, reflecting a change from an inner shelf environment to a middle- or outer-shelf environment (Appendix 5). The location of the Oligocene lowstand is inferred to lie between wackestone and calcareous sandstone (Appendix 5), a juxtaposition consistent with erosion during the lowstand. Above the Oligocene lowstand the carbonates have characteristics consistent with the flooding of the Browse Basin and

increasing water depth, as an inner-shelf depositional environment transforms into an outer shelf depositional environment (Appendix 5).

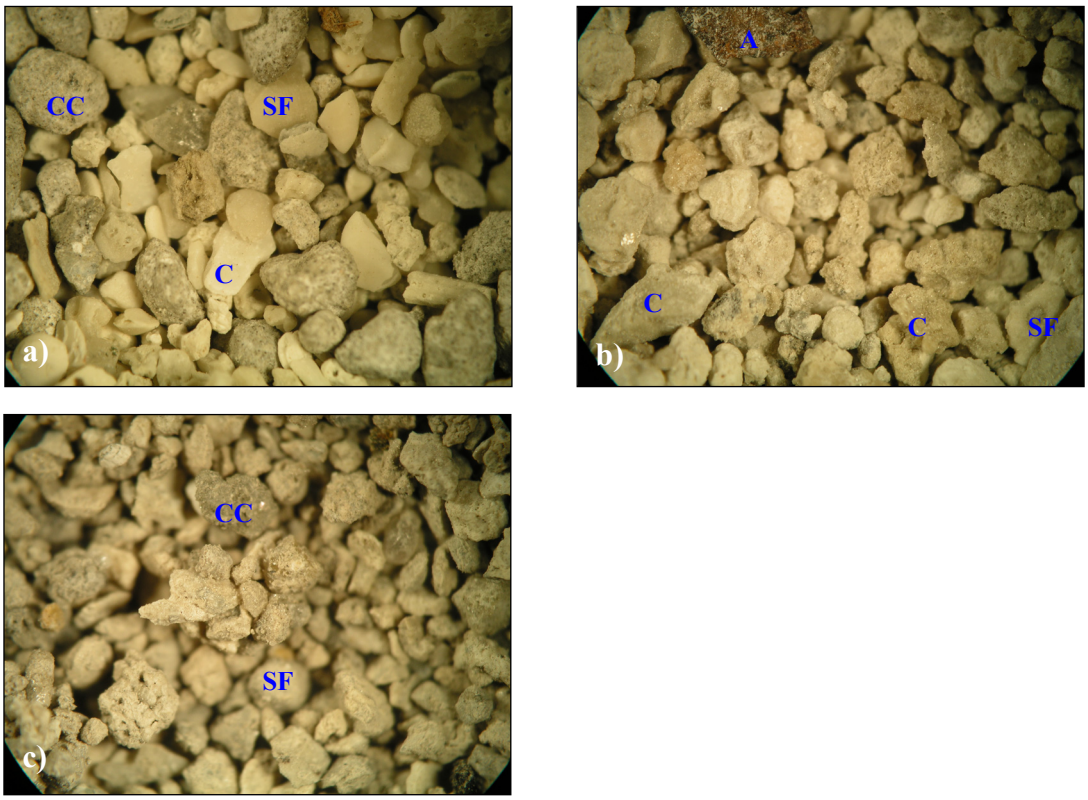

Figure 11: *Selected photomicrographs of carbonate cuttings from Echuca Shoals. Note: unless stated the field of view in all photomicrographs are 14 mm across. Labels as follows: CG – calcite grains; SF – skeletal fragments; CC – calcareous clay/silt and A – ankerite/siderite. a) Packstone from 530-535 m depth. b) Grainstone from 650-655 m depth. c) Wackestone from 820-825 m depth.*

Copernicus-ST1

Fifteen cuttings were sampled between 650 and 1250 m depth at Copernicus-1 and whilst this depth range is predominantly carbonate, three sandstone units were noted. Similar to Echuca Shoals-1, the carbonate sequence at Copernicus-1 contained minimal calcareous clay/silt and only one sample was found to be mud-supported (packstone) (Figure 12). Furthermore, trace quartz grains were found in all but two samples. Skeletal fragments range in abundance through the section, from trace to more than 90%. Pyrite and/or ankerite-siderite grains were observed throughout the section with up to 5% glauconite in the lower portion of the carbonate section. Selected photomicrographs of carbonates at Copernicus-1 are shown in Figure 12.

The lower portion of the carbonate section (1250 to 840 m) is interpreted to have been deposited in the inner shelf as the quartz ranges from 1 to 100% in abundance with >20% quartz observed in most samples. A ~40 m thick sequence of >90% intact fossils is observed from 950 to 990 m, possibly related to an ephemeral reef (Figure 12d). Similar to Echuca Shoals-1, considerable erosion is inferred during the transition to the Oligocene lowstand given the juxtaposition of sandstone overlying packstone (Appendix A5). Following the lowstand there is a general transition from sandstone to grainstone over a 100 m interval consistent with increasing relative sea level in the basin (Appendix A5).

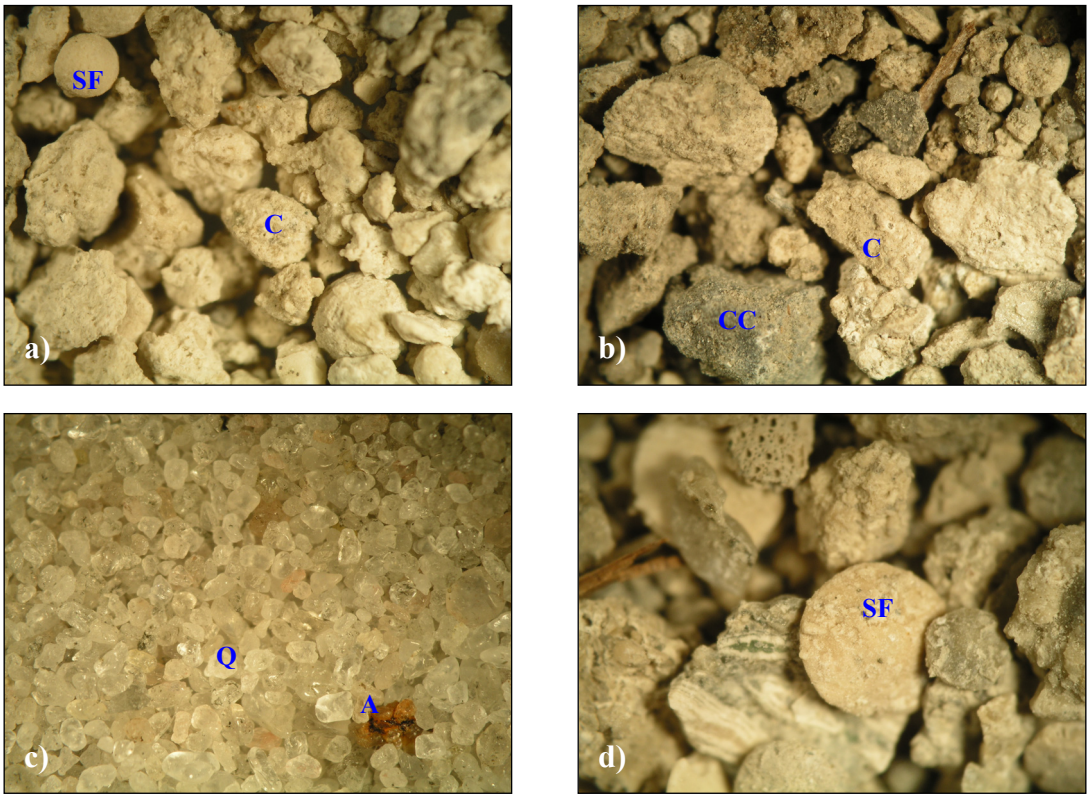

Figure 12: *Selected photomicrographs from the carbonate section of Copernicus-1. Note: unless stated the field of view in all photomicrographs are 14 mm across. Labels as follows: CG – calcite grains; SF – skeletal fragments; CC – calcareous clay/silt; Q – quartz; and A – ankerite/siderite. a) Grainstone from 650-660 m depth. b) Packstone from 750-760 m depth. c) Sandstone from 900-910 m depth. d) Fossiliferous grainstone from 980-990 m depth.*

Discorbis-1

Thirteen samples from the carbonate section of Discorbis-1 were selected for analysis; however, no samples were available between the depths of 1580 and 2046 m. The missing interval contains the transition from clastic to carbonate deposition. In general, the carbonate section at Discorbis-1 has roughly equal amounts of grain-supported and mud-supported carbonate. Quartz grains were only observed in the lower portion of the carbonate section, a zone that also contained grains of dolomite. Selected photomicrographs from Discorbis-1 are shown in Figure 13.

Deposition of the lower carbonate section is interpreted to have occurred in fluvial-deltaic and lagoonal environments as ooid- or peloid-bearing carbonates are common (Figure 13b, d). Furthermore, calcareous sandstone is intercalated in the lower carbonate section, also consistent with an inner-shelf environment. Finally, the upper carbonate section contains a transition from grainstone to calcareous mudstone consistent with increasing sea level within the Browse Basin (Appendix 5).

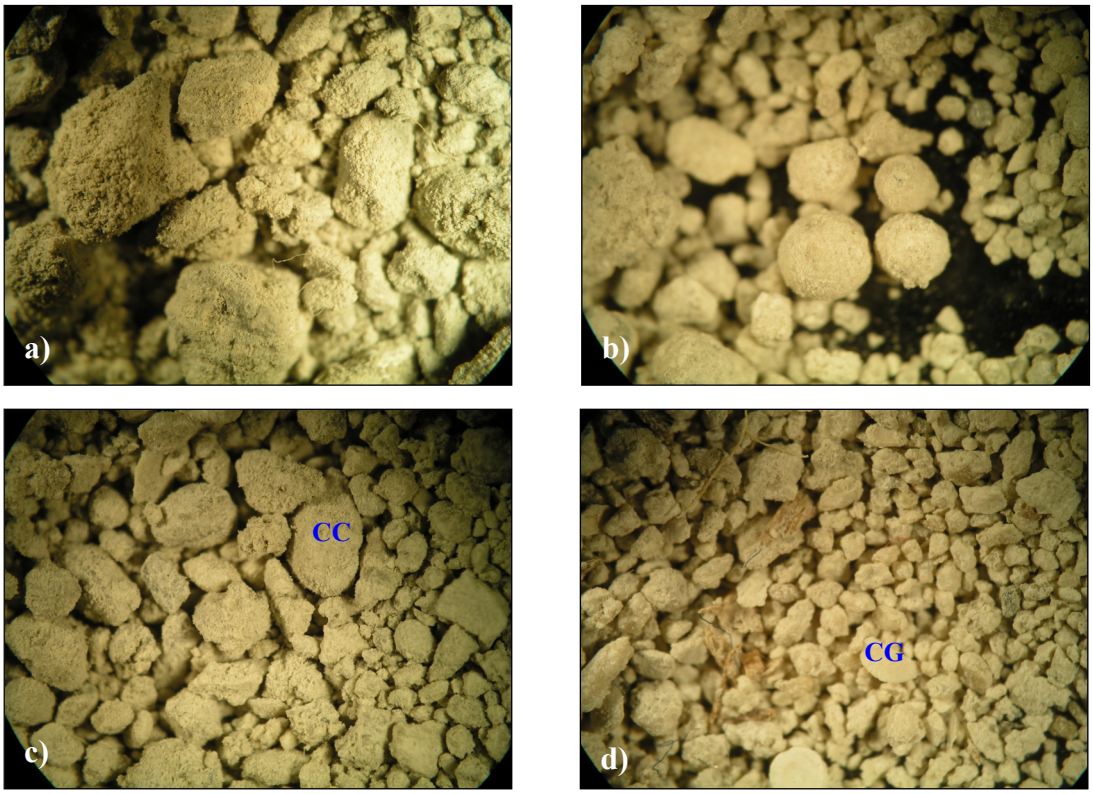

Figure 13: *Selected photomicrographs from the carbonate section of Discorbis-1. Note: unless stated the field of view in all photomicrographs are 14 mm across. CG – calcite grains; CC – calcareous clay/silt. a) Calcareous mudstone from 760-770 m depth. b) Ooids or peloids in a grainstone from 1070-1075 m depth, note here field of view is 11 mm across. c) Calcareous mudstone from 1350-1355 m depth. d) Grainstone containing occasional ooids or peloids, from 1570-1575 m depth.*

Bassett-1a

Eleven samples from the carbonate section at Bassett-1a were examined revealing the section to be largely free of quartz and dominated by grainstone and packstone. Selected photomicrographs from Bassett-1a are shown in Figure 14.

The lower portion of the section is characterised by packstones that have a decreasing quartz component up-section. This observation is consistent with a middle-shelf environment that has experienced decreasing clastic input with time. The regression to the Oligocene lowstand at Bassett-1a is marked by a transition from middle- to inner-shelf deposition. Samples from this interval contain up to 5% granule-size ankerite-siderite (Figure 14e), which may indicate periodical aerial exposure. Deposition following the Oligocene lowstand includes packages of coarse grainstones deposited in a middle-shelf environment followed by a transition to packstone near the top of the section.

Faulting associated with the Middle to Late Miocene inversion in the Browse Basin is inferred to have resulted in lithological changes at Bassett-1a (Figure 15). Cuttings recovered between 720 and 840 m include highly-crystalline grainstone intercalated in packstone that varies significantly from overlying and underlying lithologies. The grainstone is almost completely recrystallised (Figure 14d), with only rare microfossils preserved. In addition these cuttings contain up to 15% mica and up to 10% coarse-grained pyrite (Figure 14 b, c, d). The gold to black coloured mica books are distinct from clear thin muscovite sheets derived from the drilling fluid (Figure 14c). The BBHR seismic line

(175/11) shows multiple faults below Bassett-1a active during the Middle to Late Miocene (Figure 15); thus, it is postulated that the partial re-crystallisation of the packstone and secondary mineralisation resulted from fluid migration during faulting.

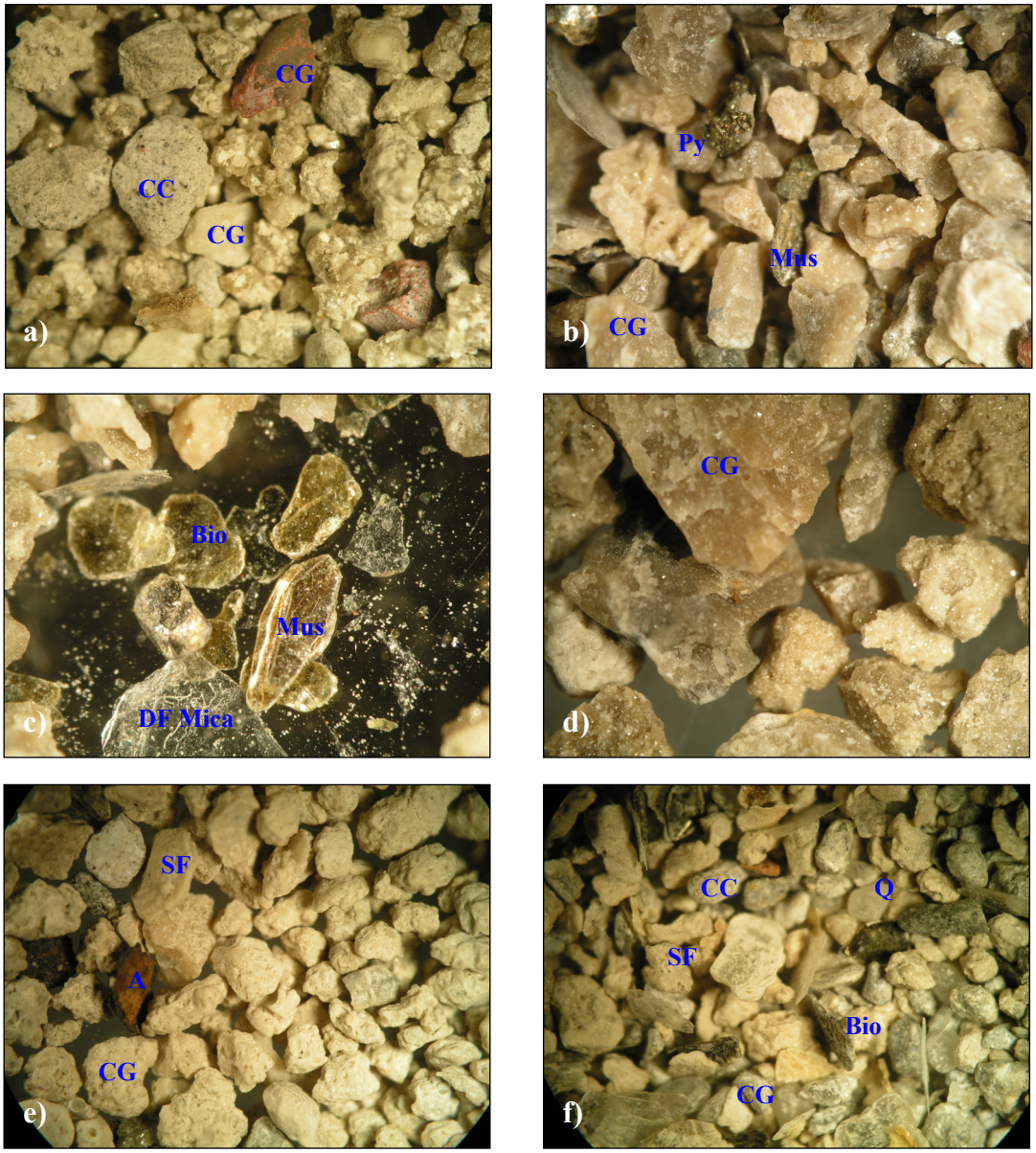

Figure 14: *Selected photomicrographs from the carbonate section of Bassett-1a. Note: unless stated the field of view in all photomicrographs are 14 mm across. Labels as follows: CG – calcite grains; SF – skeletal fragments; CC – calcareous clay/silt; Q – quartz; A – ankerite/siderite; Py – pyrite; Mus – muscovite; Bio – biotite; and DF mica – mica from the drilling fluid. a) Packstone from 740-745 m. b) Partially recrystallised grainstone from 805-810 m depth – note very coarse pyrite grains. c) muscovite and biotite booklets found within the partially recrystallised grainstone at 805-810 m depth – note clear muscovite from drilling fluid at the base of image. d) Partially recrystallised grainstone from 830-835 m depth. e) Grainstone from 1120-1125 m depth – note this sample contains up to 5% ankerite/siderite. f) Packstone from 1175-1180 m depth – note this sample also contained muscovite and biotite booklets.*

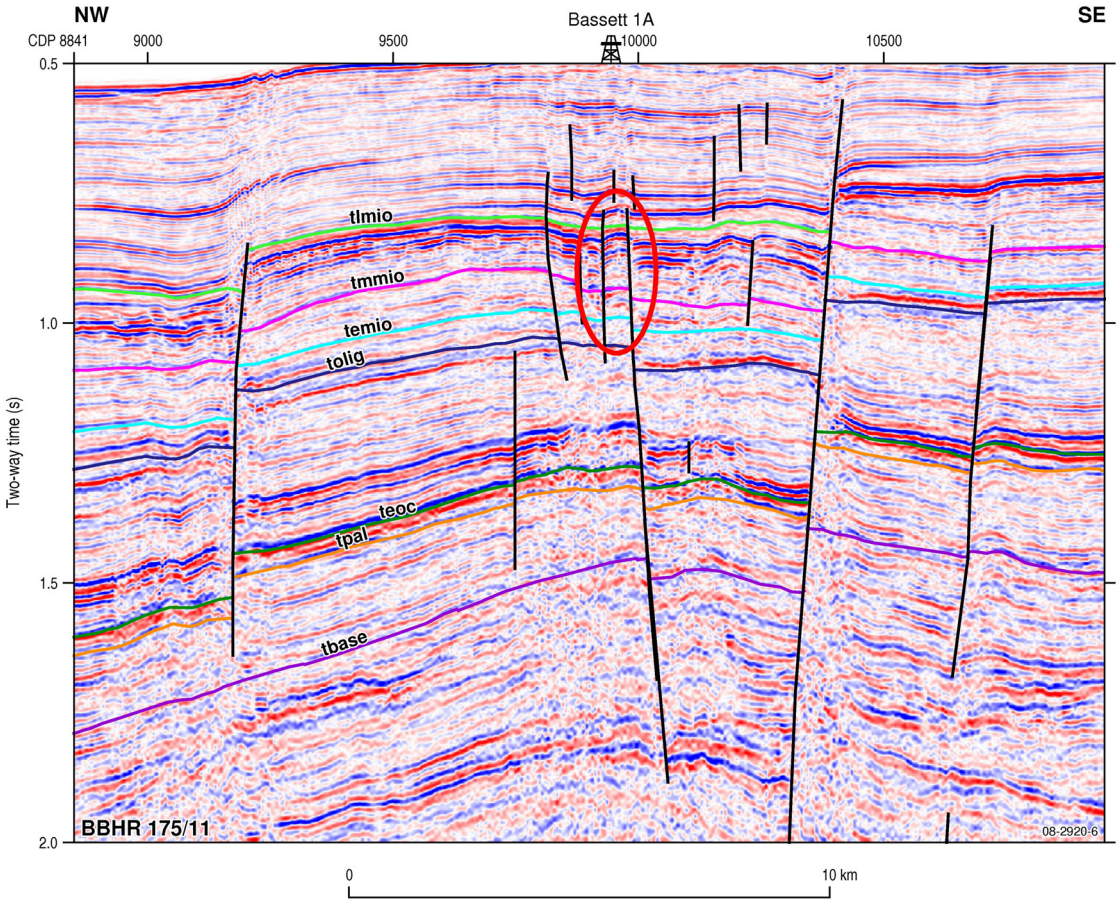

Figure 15: *Seismic Line BBHR 175/11 over Bassett 1a. This image shows the multiple faults beneath Bassett-1a, of which many were active between the Middle Miocene (Tmmio) and Late Miocene (Tlmio). Furthermore, this image shows a zone of impaired data below the Ktur horizon that is interpreted to be the result of fluid movement and cementation (AGSO Browse Basin Project Team, 1997).*

Caswell-2

Seventeen cuttings from Caswell-2 were selected for further examination. There is a significant change at Caswell-2 associated with the Oligocene lowstand as the lower section is quartz-rich and the upper carbonates are almost quartz-free. Selected photomicrographs from Caswell-2 are shown in Figure 16.

Deposition in a fluvial-deltaic and closed lagoonal environment is believed to have formed the lower carbonate, as these samples contain 30 to 70% quartz, <10% very coarse dolomite grains and <10% calcareous mud. Further evidence includes relatively high abundances of ankerite-siderite grains (Figure 16d) that may be indicative of periodical aerial exposure. Increased water depth resulted in a marked increase in skeletal fragments prior to the Oligocene. After the Oligocene lowstand there is a transition from grainstone to wackestones consistent with flooding of the Caswell Sub-basin during the transgression phase. Towards the top of the section there is a significant increase in coarse skeletal material and a decrease in the calcareous clay/silt component that may be consistent with an outer-shelf reef near Caswell-2.

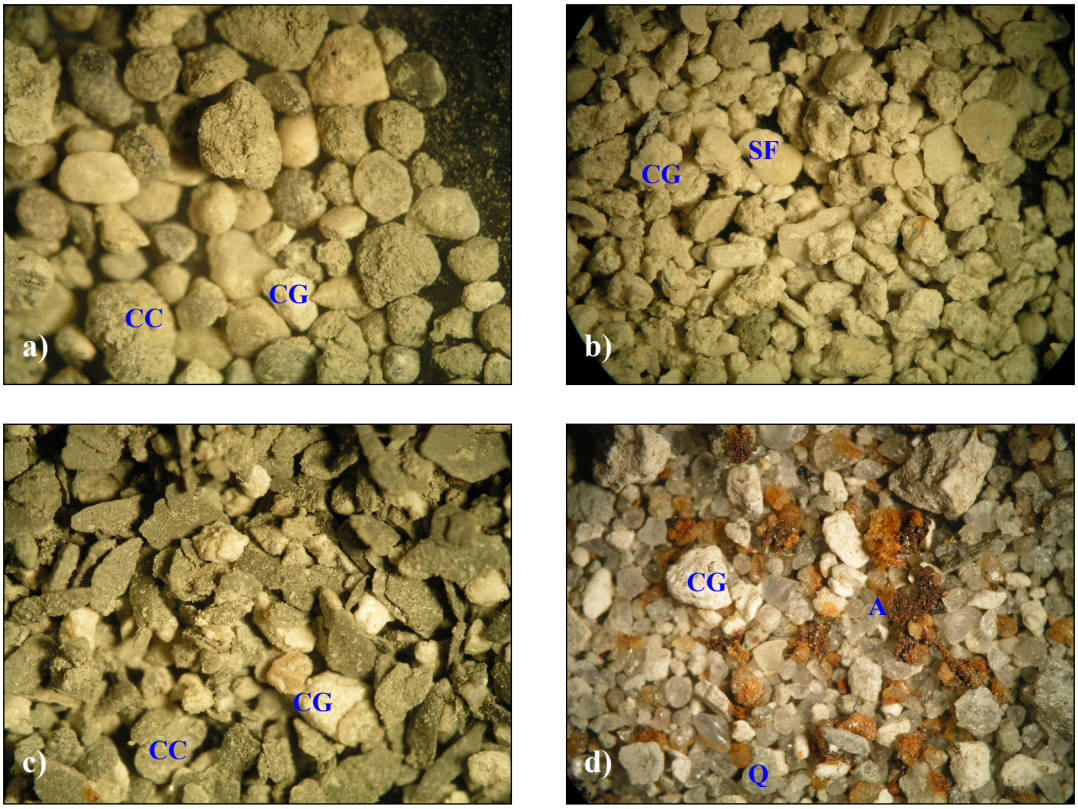

Figure 16: *Selected photomicrographs from the carbonate section of Caswell-2. Note: unless stated the field of view in all photomicrographs are 14 mm across. Labels as follows: CG – calcite grains; SF – skeletal fragments; CC – calcareous clay/silt; Q – quartz; and A – ankerite/siderite. a) Packstone from 691-695 m depth. b) Grainstone from 905-910 m depth. c) Wackestone from 1595-1600 m depth. d) Calcareous sandstone from 1950-1955 m depth – note this sandstone contains up to 15% ankerite/siderite.*

DESCRIPTION OF WIRELINE LOG RESPONSE

The gamma ray and sonic responses in the Cenozoic carbonate section were used to establish any correlative horizons, recognise density changes resulting from aerial exposure during lowstands, and reconstruct the depositional history. The log response for each of the key wells is described below and illustrated in Appendix 5. The key seismic markers used in the following discussion and in the seismic modelling section are: Tbase – Base of Cenozoic; Tpal – Top of Paleocene; Teoc – Top of Eocene; Tolig – Top of Oligocene; Temio – Top of the Early Miocene; Tmmio – Top of the Middle Miocene; and Tlmio – Top of the Miocene.

Echuca Shoals-1

Deposition of carbonates at Echuca Shoals-1 began during the Eocene; however, the transition from clastic to carbonate sedimentation can not be determined from the gamma ray response (Appendix 5). At Echuca Shoals the gamma ray response from the Oligocene and Late Miocene is on average higher than in the Paleocene and Eocene section. Furthermore, the sonic log indicates a decrease in density up-section, characteristic of a change in sediment following the Oligocene lowstand. Interestingly, the sonic log shows high frequency and high amplitude wave-forms just below the Tolig marker, possibly consistent with the development of secondary porosity and crystallisation during aerial exposure. The gamma ray response of the interval from the Late Miocene to the current sea bed reveals an initially progradational sequence with an increasing mud content up section

overlaid by an aggradational sequence. The top ~50 m of the section has a decreasing gamma ray response, with a similar response observed in almost of the wells in the Caswell Sub-basin. Superimposing the gamma ray trace onto a seismic line shows that this decrease is above the current sea-bed so is simply a sampling artefact.

Copernicus-ST1

The Paleocene to Middle Miocene interval at Copernicus-1 is represented by multiple transitions between clastic- and carbonate-dominated deposition, transitions difficult to trace using the gamma ray response. The gamma ray response from the Middle Miocene to the current seabed is consistent with a prograding sequence with an overall decreasing mud content up section.

Discorbis-1

The sandstone - carbonate boundary at Discorbis-1 could not be determined as there were no cuttings collected between 1850 and 2049 m and unfortunately no significant change in the gamma ray response over this interval. The gamma ray response is relatively unchanged over the Eocene to Early Miocene interval with a typically blocky pattern with occasional low frequency – low amplitude oscillations in the sonic log. Rhythmic progradations become recognisable in the gamma ray log in the Miocene where they continue to the current sea bed.

Bassett-1a

Carbonate deposition at Bassett-1a was initiated in the Oligocene is a blocky pattern is observed on the gamma ray trace at this time that continues to the Miocene. The sonic log shows decreasing porosity over the same interval. Progradations characterise the Miocene with an overall increase in the gamma ray response up-section. The Late Miocene interval is characterised by a significant increase in gamma ray response, up to 60 API, and an increase in porosity (note: the sonic log has a trace signal for the upper 100 m). This Middle to Late Miocene interval corresponds to partially recrystallised grainstones and a period of renewed faulting at Bassett-1a. Above this zone of high gamma ray response the progradational pattern is reinstated.

Caswell-2

The onset of carbonate deposition at Caswell-2 occurred in the Late Paleocene, recognisable by an interval of high frequency - moderate to high oscillations in the sonic response and a blocky relatively low gamma ray trace. The Eocene in that remarkable as it has the lowest sonic response seen in any carbonate sequence in the five wells that is combined with a relatively low gamma ray response. In the Early Oligocene the sonic log remains low with occasional peaks of ~45 API; however, a ~45 m zone at the base of the Miocene is characterised by high-frequency and high-amplitude oscillations. This may indicate secondary cementation and porosity destruction or formation due to periodic exposure during the Oligocene lowstand. The Miocene is characterised by a long time series of alternating progradation and aggradation, with progradation in the late Miocene resulting in a relatively high gamma ray and sonic response.

POROSITY AND PERMEABILITY OF THE CENOZOIC CARBONATES

The sealing capacity of the carbonates is contingent on low permeability; however, permeability values for the carbonates are not reported in any well-completion reports. Furthermore, visual porosity estimations were given for carbonates from sidewall cores and cuttings in only 10 wells of the Caswell Sub-basin (Table 2). Correlation of visual porosity estimations across the Sub-basin must be done with caution, particularly as visual porosity estimations may be highly subjective because the methods used for porosity estimations vary across different well sites. Nonetheless, reported visual porosity in the carbonates ranges from trace to very good and may vary from poor to good within the same well. Despite this, a rough picture of porosity within the carbonates of the

Caswell Sub-basin has emerged. Wells in the northern and eastern sections of the Sub-basin typically register moderate to good porosities (e.g., Echuca Shoals-1, Asterias-1, Heywood-1) whereas wells in the central Sub-basin typically have poor visual porosities (e.g., Caswell-2, Walkley-1, Bassett-1a) (Table 2). Sonic log porosity estimations in the central Sub-basin typically show large ranges, such as 5 to 45% in Caswell-2, which may result from secondary porosity, cementation, and/or fracturing in the carbonates.

To better determine the seal capacity of the Cenozoic carbonates carbonate samples were sent to the Australian School of Petroleum, University of Adelaide for Mercury Injection Capillary Pressure (MICP) analysis. MICP is used to determine threshold or break-through pressure used in the interpretation of the CO_2 column retention height of sealing rocks. Samples were chosen from the cuttings described in Section 4.3 where chips larger than 4 mm were found. Table 3 gives a list of the samples selected for MICP and the height of CO_2 column (m), and the full report is included in the Appendix 4. As analyses were conducted on dried unwashed bulk cuttings the clay minerals in the cuttings may have experienced some structural degradation resulting in lower than expected column heights. Samples with the best seal capacity (column height) include a mudstone, wackestone and a well cemented to recrystallised grainstone, whilst grainstone and packstone lithologies returned very low to moderate column heights. Calculated porosities ranged from 15% to 37% in line with reported log porosity estimations (Table 2).

Table 2: Porosity Values. * Values may not be accurate as the sandstone has an average log porosity of 51%.

WELL	DEPTH (m)	AGE	LITHOLOGICAL DESCRIPTION	VISUAL POROSITY ESTIMATIONS	LOG POROSITY ESTIMATIONS
Asterias-1	508 - 852	Miocene to Recent	Bioclastic calcarenite (Grainstone)	Poor to moderate	
	930 - 1086	Eocene	Bioclastic calcarenite (Grainstone)	Good	
	1465 - 1495	Paleocene to Eocene	Calcarenite (Grainstone)	Moderate	
	1587 - 1624	Paleocene to Eocene	Dolomite	Poor to Good	
	1914 - 1936	Paleocene	Calcarenite (Grainstone)	Poor	
Bassett-1a	717 - 735	Miocene	Calcarenite		30 - 39%
	735 - 1120	Middle Eocene to Miocene	Calcarenite (Grainstone)	Trace to Poor (intergranular & vugular)	745 - 986 m: 10 - 34%; 986 - 1120 m: 23 - 30%
Heywood-1	377 - 882	Middle Miocene to Pliocene	Calcarenite	Moderate to Very Good	
Prudhoe-1	512 - 750	Middle Miocene to Pliocene	Calcarenite (Packstone - Grainstone)	Poor to Good (intraskeletal & intergranular)	
	785 - 816	Eocene	Calcarenite (Grainstone)	Trace to Very Good (intraskeletal)	
Brewster-1	638 - 720	Middle to Late Miocene	Calcisiltite (Wackestone)	15 - 20%	14 - 33%
	720 - 900	Middle to Late Miocene	Calcarenite (Packstone - Grainstone)	5 - 10% (intergranular & vugular)	14 - 33%
Brewster-1	900 - 950	Middle to Late Miocene	Calcarenite (Packstone - Grainstone)	5 - 10% (vugular)	14 - 33%
	950 - 1018	Middle to Late Miocene	Calcarenite (Packstone)	5 - 10% (intergranular)	14 - 33%
	1275 - 1285	Middle to Late Eocene	Calcarenite (Grainstone)	5 - 25%	
Rob Roy-1	427 - 567	Miocene to Pliocene	Calcarenite (Grainstone)	Poor to Good	Average 42%*
Caswell-2	775 - 825	Late Miocene	Marl grading to calcarenite	Trace to 15%	
	825 - 1660	Miocene to Late Miocene	Calcarenite (Packstone to Grainstone) to Calcisiltite		23 - 45%
	1952 - 2079	Middle Eocene	Calcisiltite		5 - 45%
Walkley-1	809-1198	Miocene	Calcarenite (Grainstone)	Poor to moderate	
	1198 - 1566	Miocene	Calcilutite and Calcarenite (Wackestone and Packstone)	Poor	
	1566 - 1608	Miocene	Calcarenite (Grainstone)	Poor	
	1861 - 1960	Palaeogene	Dolomitic calcarenite and calcilutite	Poor to Good	
Yampi-1	545 - 670	Middle Miocene to Pliocene	Dolomite	5 - 10% (intergranular)	
	779 - 789	Middle to Late Miocene	Calcarenite (Grainstone)	15% (intergranular)	

Table 3: Samples selected for MICP.

WELL	DEPTH (m)	LITHOLOGY	HEIGHT OF CO_2 COLUMN (M)
Discorbis-1	760 - 770	calcareous mudstone	236
	1350 – 1360	calcareous mudstone	6
Copernicus 1	750 - 760	packstone	82
	780 – 790	grainstone	56
	810 – 820	grainstone	56
Caswell 2	795 – 800	wackestone	115
Bassett 1a	830 – 835	partially recrystallised grainstone	480

PALAEOGEOGRAPHY OF THE CARBONATES

A preliminary interpretation of the palaeogeographical environment of carbonate deposition was undertaken to better evaluate the distribution of a potential seal. The broad depositional environments have the following characteristics. Deposition within the fluvial-deltaic environment predominantly involves clastic material, coarse sands through to non-calcareous silt/clays that are typically deposited in fluvial deltas. Furthermore, calcareous mudstones, wackestones and packstones that contain a high proportion of ooids-peloids, dolomite and/or clastic material are interpreted to have been deposited within low energy lagoons. Inner-shelf is a zone wherein clastic and carbonate layers are intercalated in relatively small packages, or where carbonates contain relatively high proportions of sand. Deposition in the middle shelf is carbonate dominated, with moderate energy producing relatively clay/silt free carbonates, such as grainstones. Finally, deposition within the outer shelf environment is dominated by carbonates with a moderate to high proportion of calcareous clay/silt, such as wackestones and mudstones.

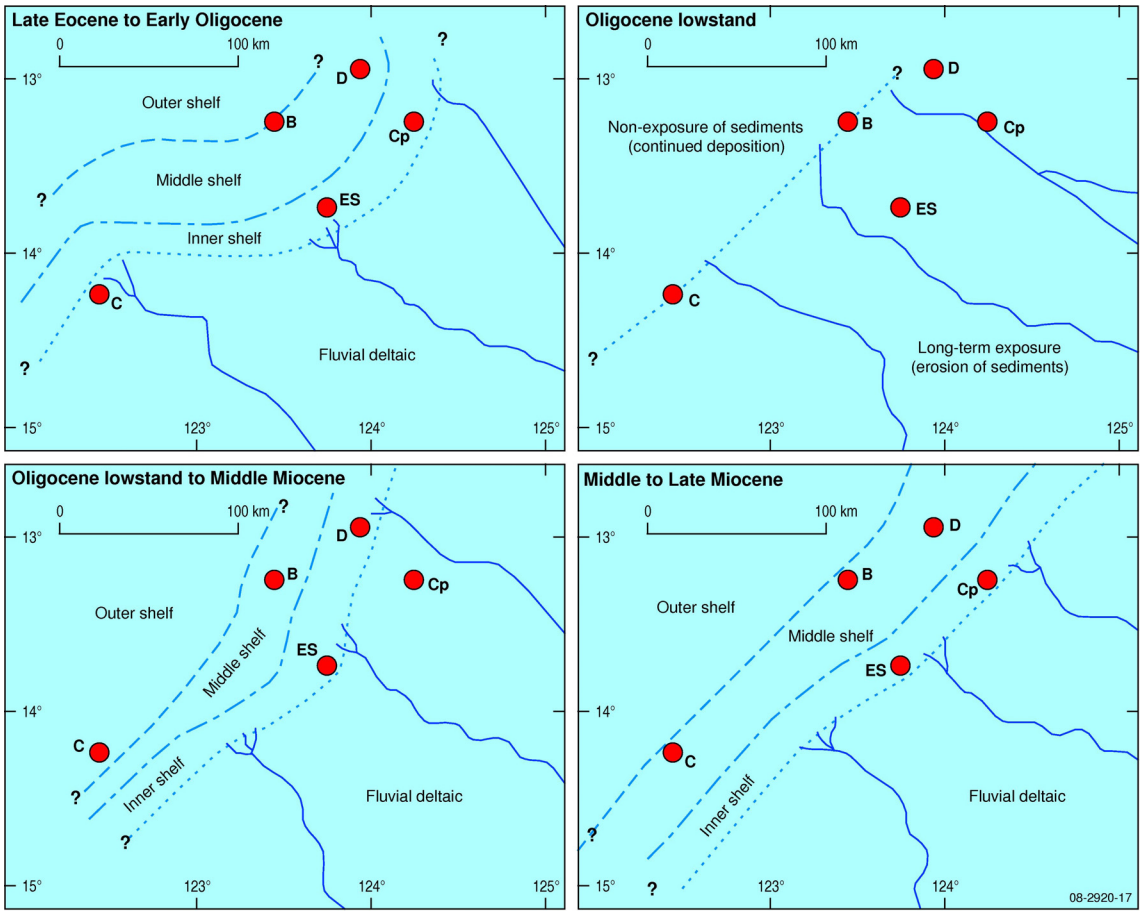

Figure 17: *Palaeographic interpretations of four time slices during the Cenozoic in which significant carbonate deposition occurred. In addition, the approximate regions of deposition, non-deposition and erosion during the Oligocene low stand are delineated. These interpretations are based on information gleaned from the well completion reports, observations from well cuttings and the wireline log responses. Abbreviations for the wells as follows: D – Discorbis-1; Cp – Copernicus-1; B – Bassett 1a; ES – Echuca Shoals-1; and C – Caswell-2.*

The palaeogeographical interpretation in Figure 17 was compiled using information in well-completion reports, well-cutting descriptions and wire line log responses. Four time slices are represented in Figure 17, with the four different palaeodepositional environments delineated. The

depositional conditions in the Caswell Sub-basin during the Pliocene to present day are believed to reflect deeper water as the coastline shifted to its current position. Thus, at Echuca Shoals-1 and Copernicus-1 carbonate deposition is inferred to be typical of the middle shelf, such as grainstones and packstones, whereas Discorbis-1, Caswell-2 and Bassett-1a now lie in the outer shelf where carbonate deposits have relatively high clay/silt contents.

SEAL WITH THE HIGHEST POTENTIAL IN THE CENOZOIC CARBONATE SECTION OF THE CASWELL SUB-BASIN

In terms of a CO_2 seal, the best Tertiary carbonates are located within the central Caswell Sub-basin. These carbonates have the lowest porosity values and the thickest carbonate sections. Moreover, the central Caswell Sub-basin is more likely to have thicker sections of carbonate with high micrite content (mudstones and wackestones) which has have been shown by MICP analysis to have better seal capacity than carbonates with low micrite content (grainstones and packstones). In addition, palaeogeographic reconstructions indicate that carbonates in this area did not experience sustained aerial exposure during the Oligocene lowstand or Pliocene/Holocene lowstands. The probability of secondary porosity and karstic features within these carbonates is therefore lower than in carbonates in the eastern Sub-basin that appear to have had fluvial and aerial erosion.

Seismic Interpretation of the Cenozoic Sandstones and Carbonates

To facilitate interpretation of the Cenozoic evolution of the Caswell Sub-basin, depositional features, unconformities, unit thickness and clastic versus carbonate depositional boundaries were identified on five seismic lines (locations shown in Figure 18). These seismic lines were collected as part of the Browse Basin High Resolution seismic survey that was carried out in 1996. Four of the selected seismic lines run roughly perpendicular to the current coastline, including: BBHR-175/12 which passes the wells of Productus-1, Asterias-1 and Kalyptea-1; BBHR-175/11 that runs through Buccaneer-1 and Bassett-1; BBHR-175/10 which goes through Rob Roy-1 and Echuca Shoals-1; and s119_119-05 which runs through Yampi-1, Walkley-1 (near Caswell-2) and North Scott Reef-1. A fifth seismic line lies roughly parallel to the coastline is located near the centre of the Caswell Sub-basin (BBHR-175/15), and passes through Delta-1, Discorbis-1, Bassett-1 and Walkley-1. Key features from interpreted seismic lines are displayed and summarised in this section.

Significant observations regarding Cenozoic deposition and structure throughout the Caswell Sub-basin include:

- The Cenozoic units thicken substantially towards the northwest, from ~0.5 seconds near the Yampi Shelf to approximately ~2.3 seconds at the boundary of the Scott Plateau and Seringapatam Sub-basin. Note: in the Cenozoic sequence 1.0 second is equivalent to roughly 1200 to 1500 m (determined from seismic lines and well-completion reports at Rob Roy-1, North Scott Reef-1, Bassett-1a and Walkley-1). Without a depth conversion the sequence will be referred to in time.
- The BBHR-175/15 seismic line reveals that the thickness of the Cenozoic sequence varies from the southwest to the northeast, with Bassett-1a situated over a relatively thin package of Cenozoic deposits (~1 sec) and Caswell-2 located over a relatively thick package of Cenozoic material (~1.5 sec). This variation appears to correlate with deformation within the Caswell Sub-basin, as the area around Bassett-1a was folded upwards between the Cretaceous and Middle Miocene.
- Deformation of the Cenozoic sequence is considerably more prevalent in the north-east Caswell-Sub-basin. Faulting during the Miocene is observed near Bassett-1a (Figure 19), as is folding of

Pliocene to Recent carbonates (Figure 20). Furthermore, many faults intersect the sea floor in the northeast Caswell Sub-basin (Figure 21).

- The characteristic seismic expression of the Cenozoic sands ranges from chaotic to moderately continuous and is low to moderate amplitude (Figure 22). In contrast, the seismic expression of the carbonates is typically of high continuity and moderate to high amplitude (Figure 22).

The following section describes in further detail depositional and deformational features found within seven key time periods identified within the Cenozoic units of the Caswell Sub-basin.

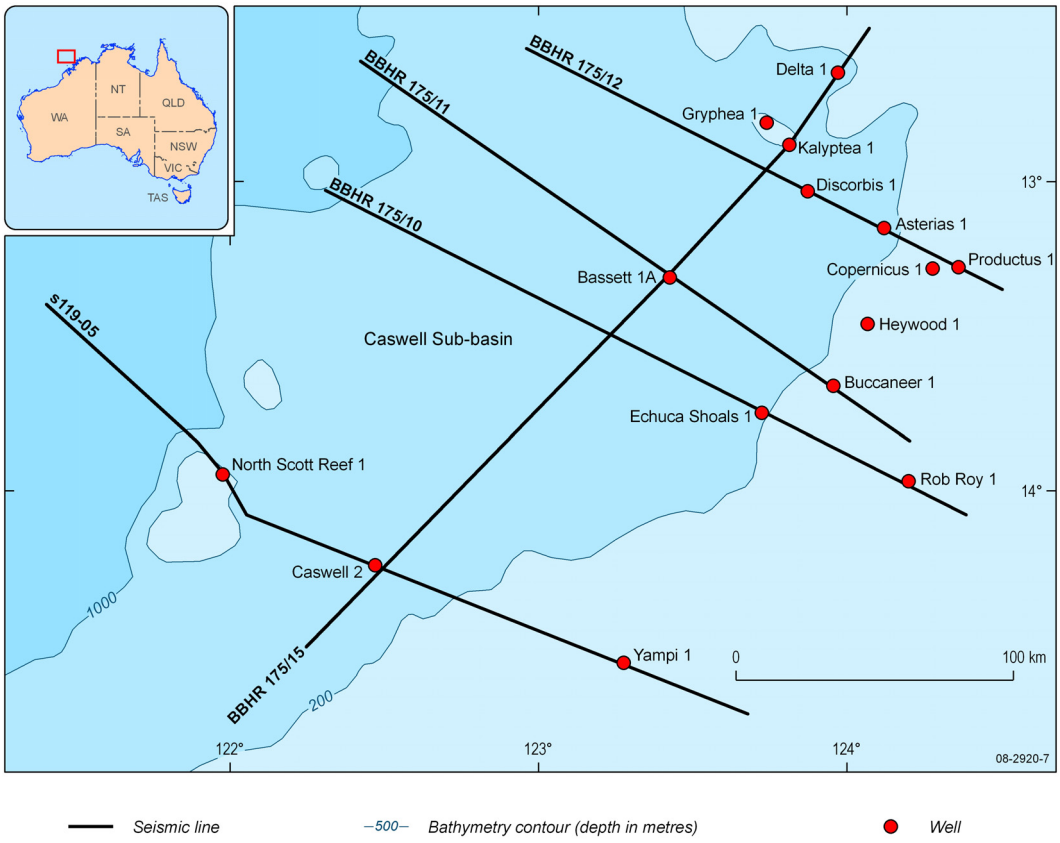

Figure 18: *Seismic lines that are described in this section and key wells in the Caswell Sub-basin.*

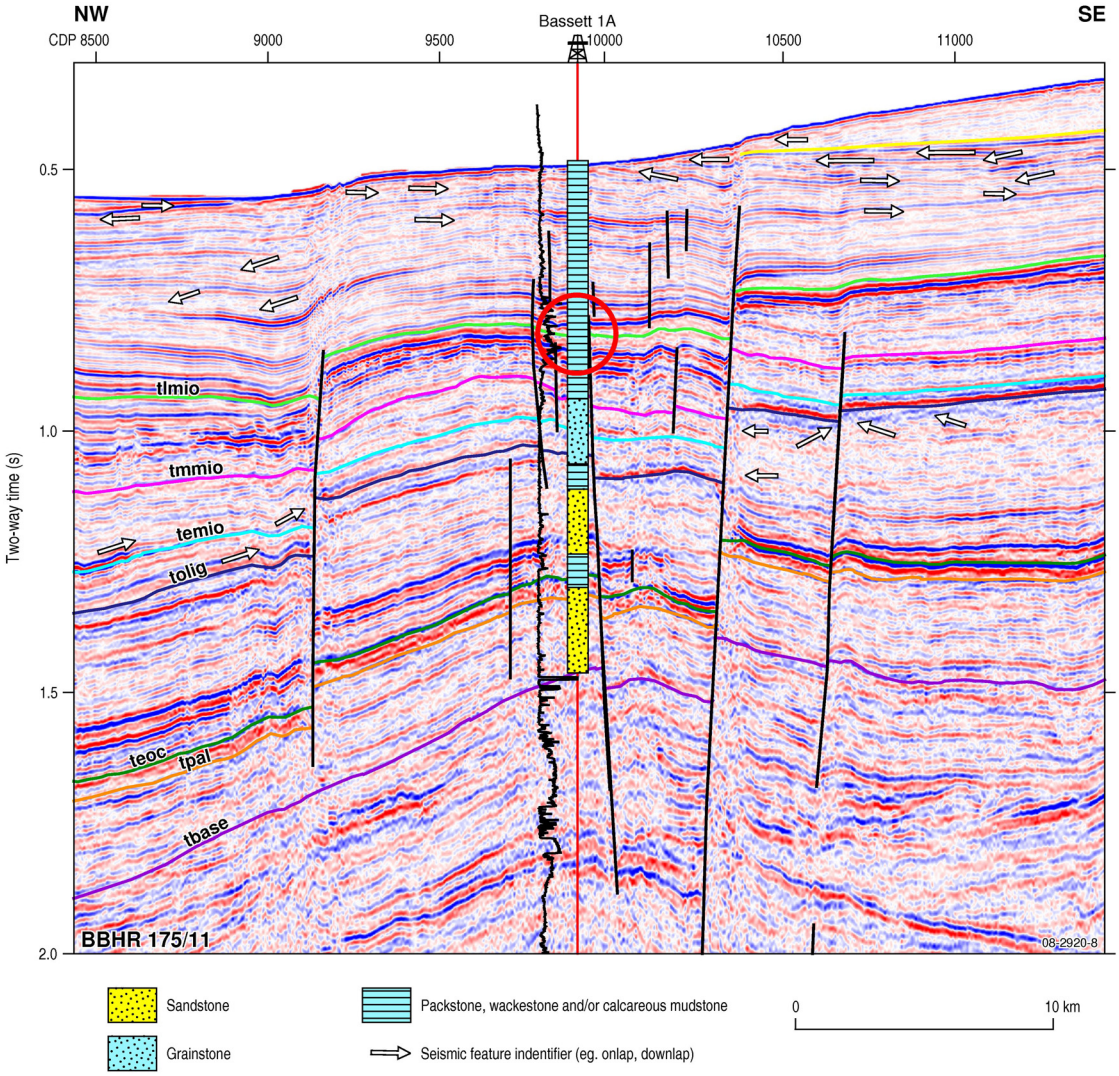

Figure 19: *Middle shelf location on seismic line BBHR-175/11. Faulting in the Middle to Late Miocene around Bassett-1a. Note the change in gamma ray response (red circle) in the carbonates of this time period. This figure also shows an erosion surface formed during the Pliocene to Holocene interval.*

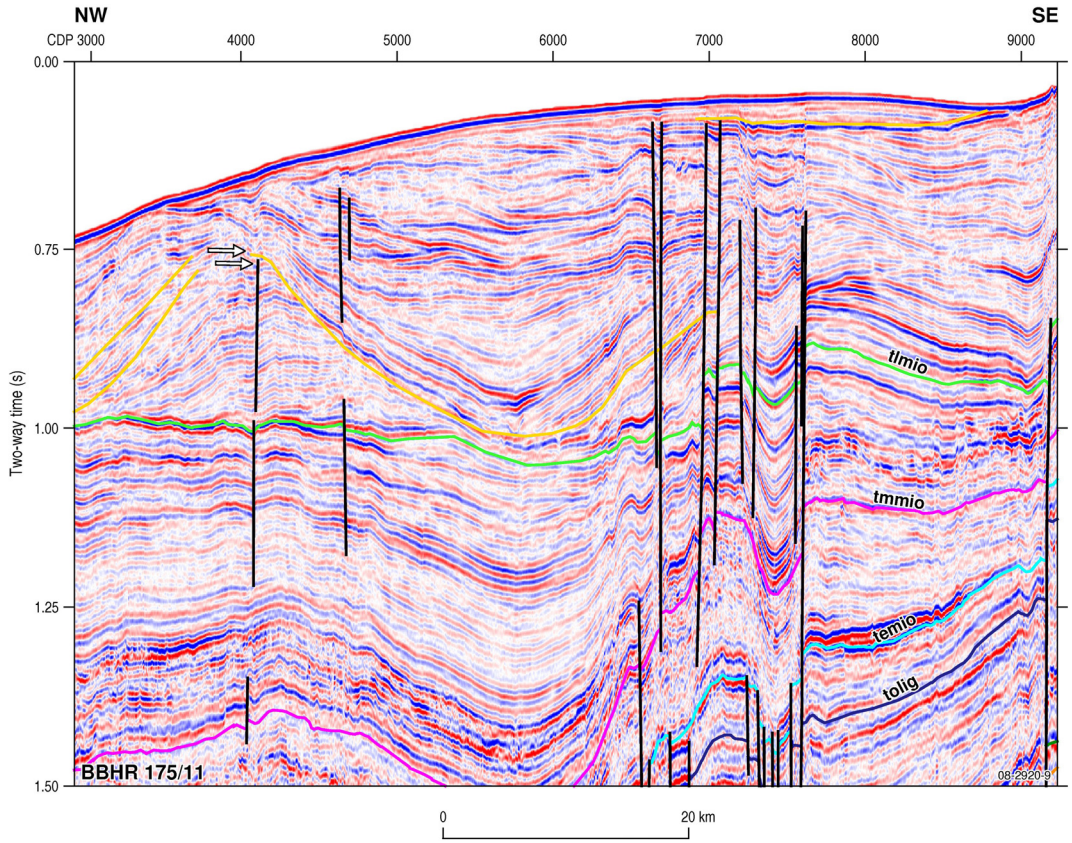

Figure 20: *Outer-shelf location on seismic line BBHR-175/11. Folding and subsequent infilling of accommodation space by carbonate material during the Late Miocene to Holocene. Also note the considerable faulting of Miocene and Holocene deposits.*

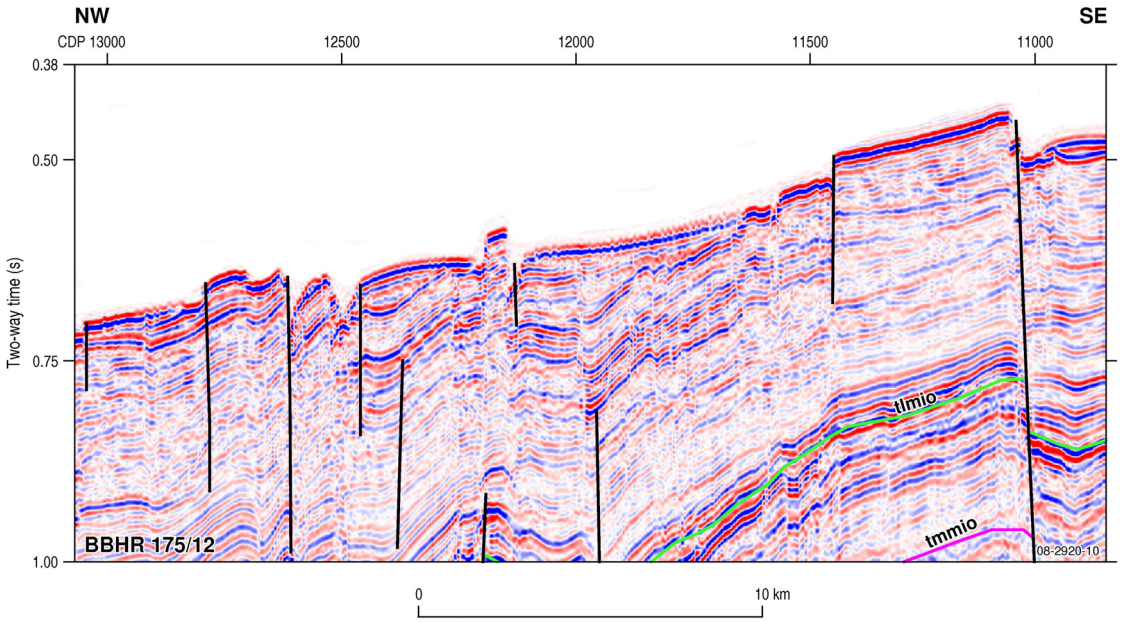

Figure 21: *Middle-shelf location on seismic line BBHR-175/12. Faulting of the present-day seafloor in the northern Caswell Sub-basin.*

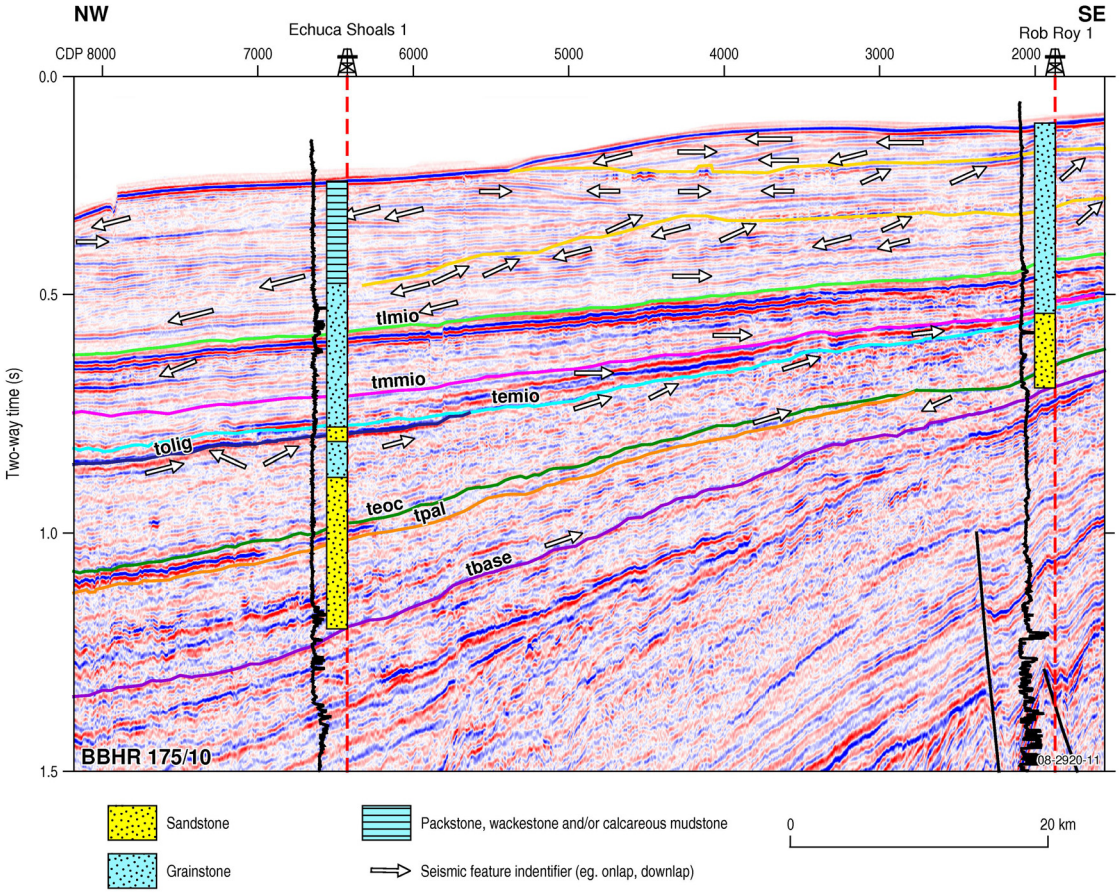

Figure 22: *Part of the BBHR-175/10 seismic line near Echuca Shoals and Rob Roy. Demonstrating the characteristic seismic expression of the Cenozoic sandstones and carbonates, this figure also illustrates several key features: (1) two erosion surfaces in the Pliocene and Holocene (yellow lines); (2) subtle progradational features visible below the lower Pliocene/Holocene erosion surface; and (3) truncations associated with the Oligocene lowstand.*

PALEOCENE (TBASE TO TPAL)

Paleocene deposition within the Caswell Sub-basin was very limited in the south-east with less than 0.1 seconds of material identified on the seismic lines (Figure 22), and towards the Yampi Shelf this unit pinches out. The Paleocene unit thickens to the northwest and has a two-way travel time of 0.25 seconds at the shelf edge (Figure 22). During this time period, carbonate deposition occurred in the northeast and northwest of the Sub-basin (e.g., Productus-1, North Scott Reef-1) whereas clastic sedimentation dominated in the rest of the Sub-basin reflecting the position of the coastline at the time. Aggradation of sediments occurred throughout most of the basin with slope fans (Figure 23) and sigmoidal prograding wedges identified at the Sub-basin outer margin.

Faults penetrate the Paleocene sediments in most of the Sub-basin with some of these faults reaching the current seabed. Furthermore, Paleocene sediments near Bassett 1a are folded, a deformation process that continued into the Middle Miocene (Figure 19). Significantly the area surrounding and upslope from Caswell-2 does not have faults that penetrate the Paleocene unit (Figure 24).

EOCENE (TPAL TO TEOC)

Deposition during the Eocene appears to have been relatively limited, with the Tpal seismic horizon onlapping onto the Teoc seismic horizon ~30 km southeast of Echuca Shoals-1 (Figure 22) and the thickest section is only 0.13 seconds at the shelf margin. During this time period, clastic sedimentation dominated in the central and south-eastern Sub-basin (Figure 24, 25) with carbonate sedimentation at the north-western margin. Deformation of Eocene sedimentary units closely resembles that of the Paleocene units.

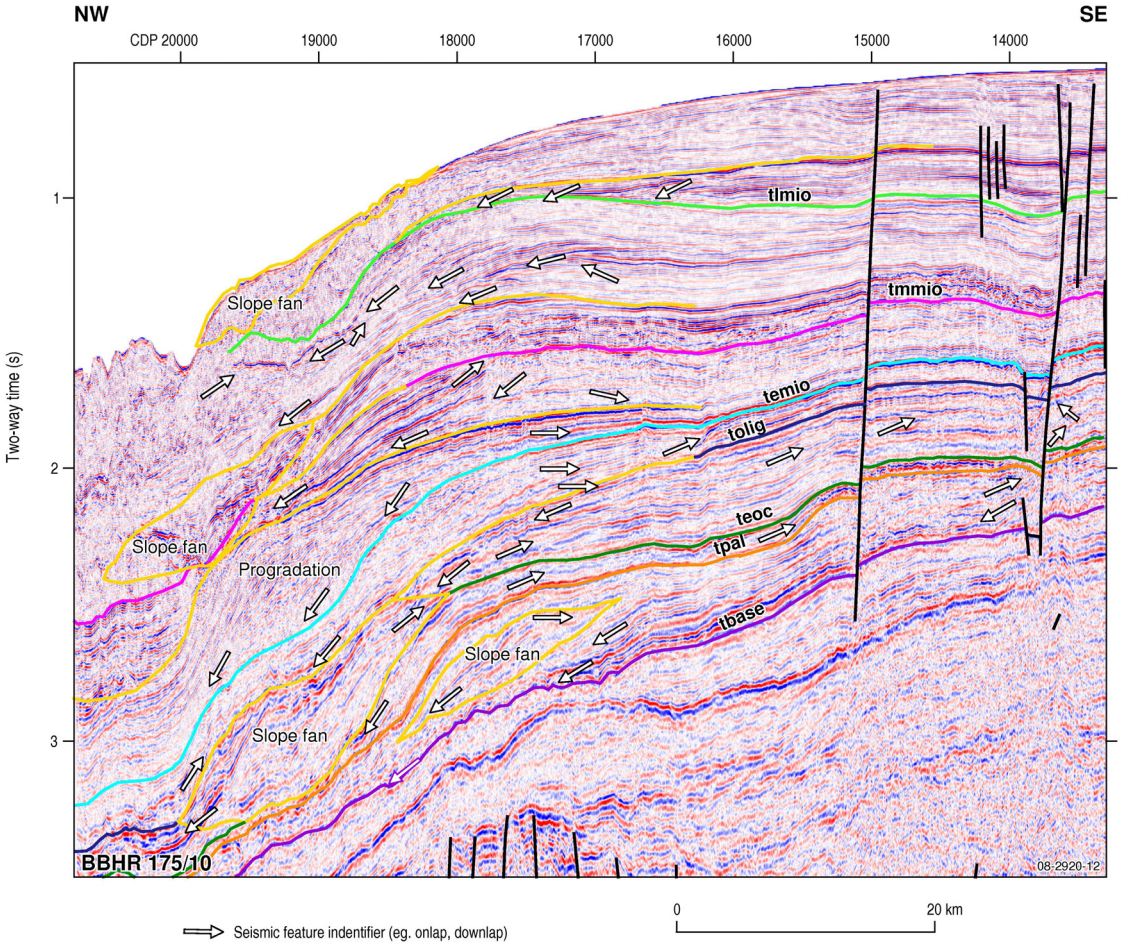

Figure 23: *BBHR 175/10 seismic line. Cenozoic depositional features observed at the outer shelf of the Caswell Sub-basin.*

OLIGOCENE (TEOC TO TOLIG)

Rates of deposition during the Oligocene (prior to the Oligocene lowstand) were significantly higher than during the Eocene, with 0.2 seconds of sediment at Echuca Shoals in the south-eastern Sub-basin and 0.45 seconds at the north-eastern margin. In the Sub-basin, regions of clastic and carbonate deposition remained similar to Eocene deposition, although deposition here occurred at higher rates due to increased sediment supply. Slope fans are recognised at the shelf margin. Aerial exposure during the Oligocene lowstand is recognised on seismic lines by erosion that truncates sequences and channel features. These erosional features are predominantly found southeast of Bassett-1a, Caswell-2 and Kalyptea-1 (Figure 19, 24 and 26), supporting the placement of the zone dividing marine deposition and aerial erosion of sediments in Figure 17.

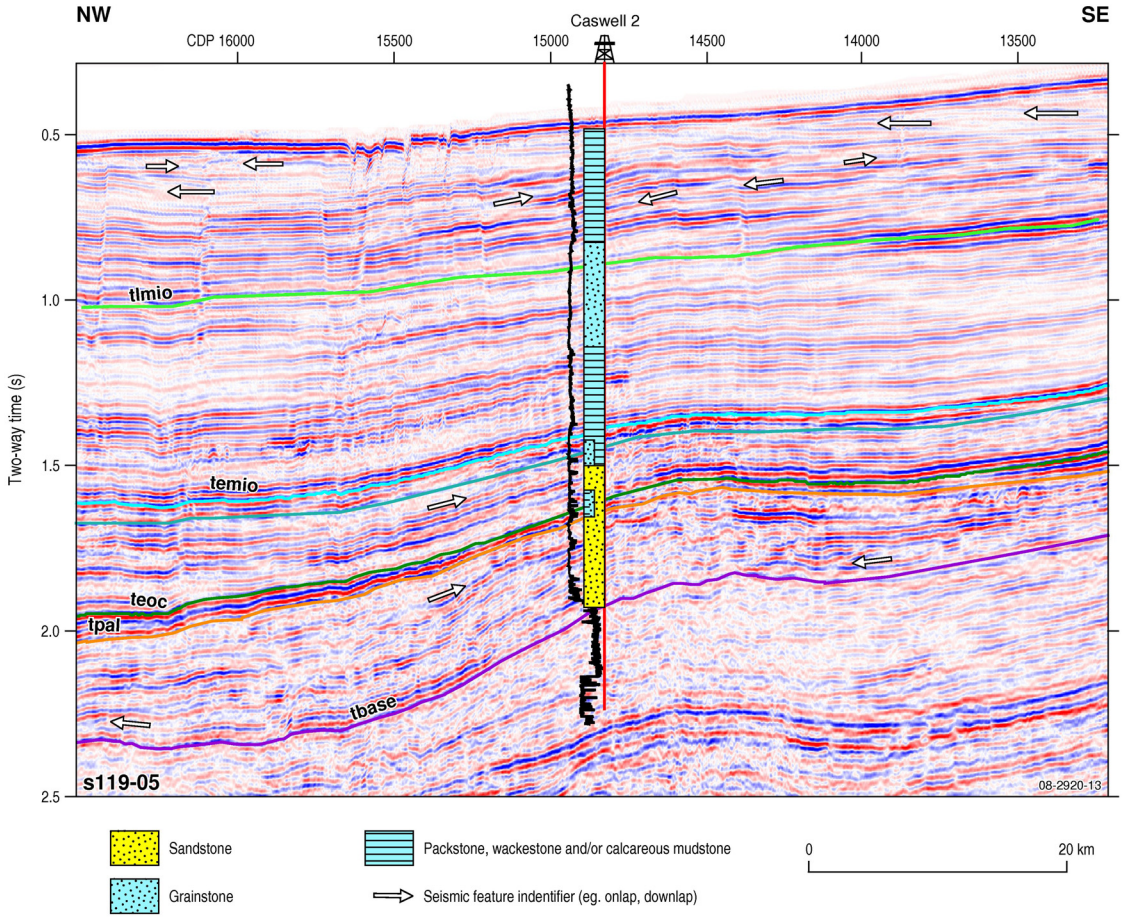

Figure 24: *Seismic line s119-05. The seismic character of Cenozoic sediments at Caswell-2.*

EARLY MIOCENE (TOLIG TO TEMIO)

The Early Miocene period saw relatively low rates of deposition in the Caswell Sub-basin. Nonetheless, minor deposition during this period is recorded southeast of Echuca Shoals-1 and Productus-1 (Figures 22 and 26) with sediment thickness increasing northwest up to 0.3 seconds. This period corresponds to the onset of significant carbonate deposition within the Sub-basin, with carbonates now dominating over clastic sedimentation everywhere except the most northern and eastern parts of the Sub-basin. At the shelf margin, slope fans are identified as well as the base of sigmoidal prograding wedges (Figure 23).

MIDDLE MIOCENE (TEMIO TO TMMIO)

Deposition during the Middle Miocene does not differ substantially from the Early Miocene; however, movement of the coastline eastwards and a decrease in clastic sedimentation meant that carbonate deposition was now occurring throughout the Sub-basin. This unit ranges from less than 0.1 second in the south-eastern basin up to ~0.5 seconds in the northwest. At the outer shelf sigmoidal prograding wedges are identified (Figure 23) but over the rest of the basin aggregation predominates (Figure 22).

LATE MIOCENE (TMMIO TO TLMIO)

The Late Miocene period saw a significant increase in the rate of carbonate deposition that continues through to the Holocene. Late Miocene thicknesses range from 0.15 seconds near the Leveque Shelf to 0.5 seconds in the middle to outer shelf. The region around Caswell-2 records some of the greatest thicknesses of carbonate sedimentation during this period. Parallel seismic facies are most characteristic of this time period, indicating that aggradation, rather than progradation, dominated throughout the basin at this time. At the shelf margin, slope fans and sigmoid prograding wedges are observed (Figure 23).

During the Late Miocene, deformation northwest of Bassett-1a produces increased space for deposition (Figure 20), a trend that continues into the Pliocene/Holocene. At the site of Bassett-1a, deformation predominantly involved renewed faulting, with four faults in close proximity to the well site (Figure 19). As noted earlier, this zone of faulting corresponds with a zone of partially recrystallised carbonates containing significant quantities of mica and pyrite.

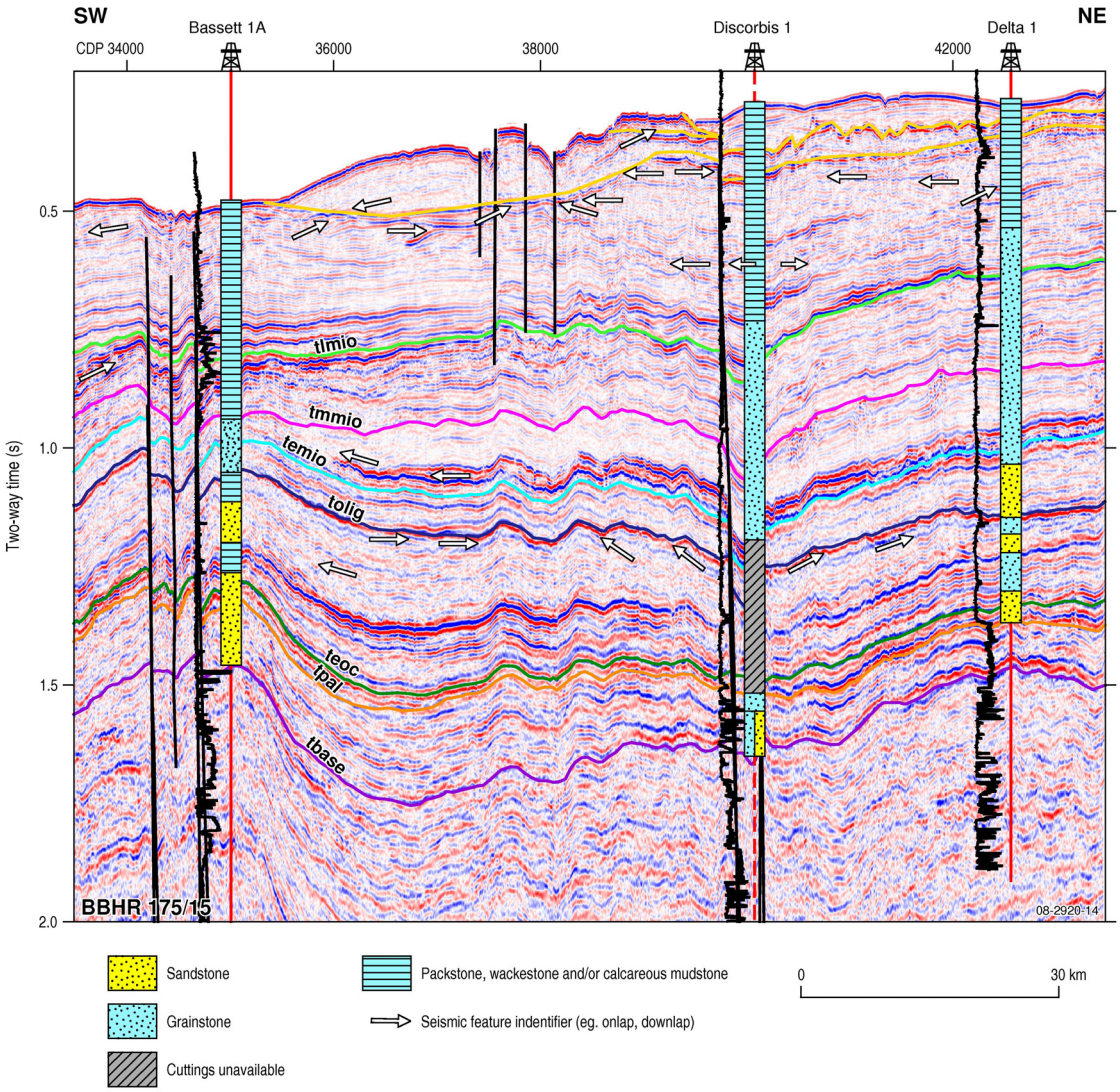

Figure 25: *BBHR-175/15. A seismic line running roughly parallel to the current coastline illustrating the changing seismic character at Bassett-1a, Discorbis-1, and Delta-1.*

PLIOCENE TO HOLOCENE (TLMIO TO SEABED)

This time period is undifferentiated and includes all deposition during the Pliocene to the present day (Holocene). Across the Sub-basin the thickness of deposition during this period is relatively consistent, now located on the middle to outer shelf, with 0.3 seconds in the southeast and 0.5 seconds in the central and northwest basin. Whilst minor oblique progradations are observed in this interval (Figures 22 and 27), aggradation of carbonates dominated throughout the majority of the basin during this time period and parallel, highly continuous and moderate amplitude reflections are most characteristic (Figures 19, 24 and 26). At the shelf margin some slope fans are observed.

The seismic lines distinctly show at least two erosional unconformities in this interval, with erosional and highly irregular surfaces observed in the south-eastern and north-eastern sections of the Sub-basin (Figures 19, 22, 25 and 26). Above the most recent erosional surface, the sediments often have remarkably different reflection characteristics as compared to the layer below, typically very low amplitude and slightly chaotic (Figures 19 and 27). The chaotic nature of the seismic package infers deposition in a medium to high energy environment, similar to what may be seen in a submarine fan deposit or a mass transport deposit.

Deformation during this time includes continued subsidence possibly associated with faulting northwest of Bassett-1a and significant faulting is observed in the north-east Caswell-Sub-basin. Furthermore, many faults intersect the sea floor in the northeast Caswell Sub-basin (Figure 21).

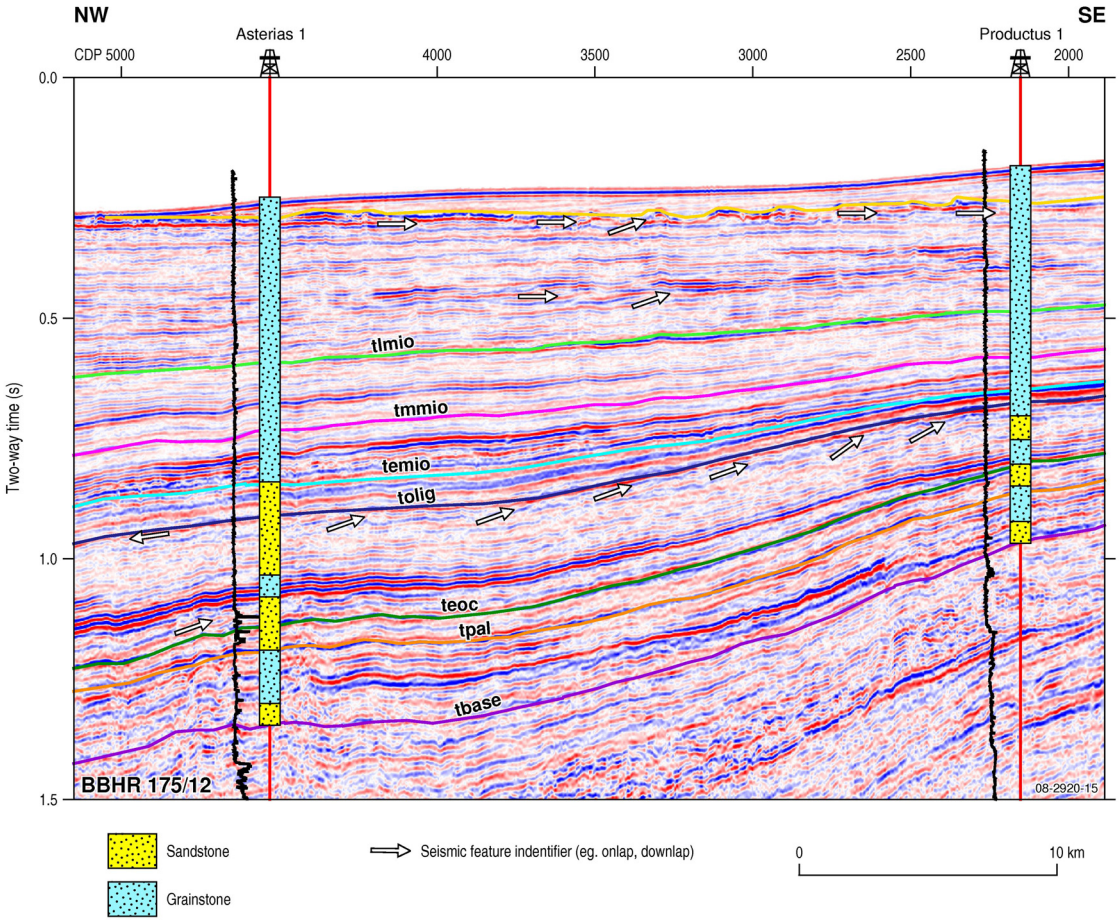

Figure 26: *BBHR-175/12. Erosion surfaces observed in the south eastern Caswell Sub-basin, one during the Pliocene to Holocene and the second associated with the Oligocene lowstand.*

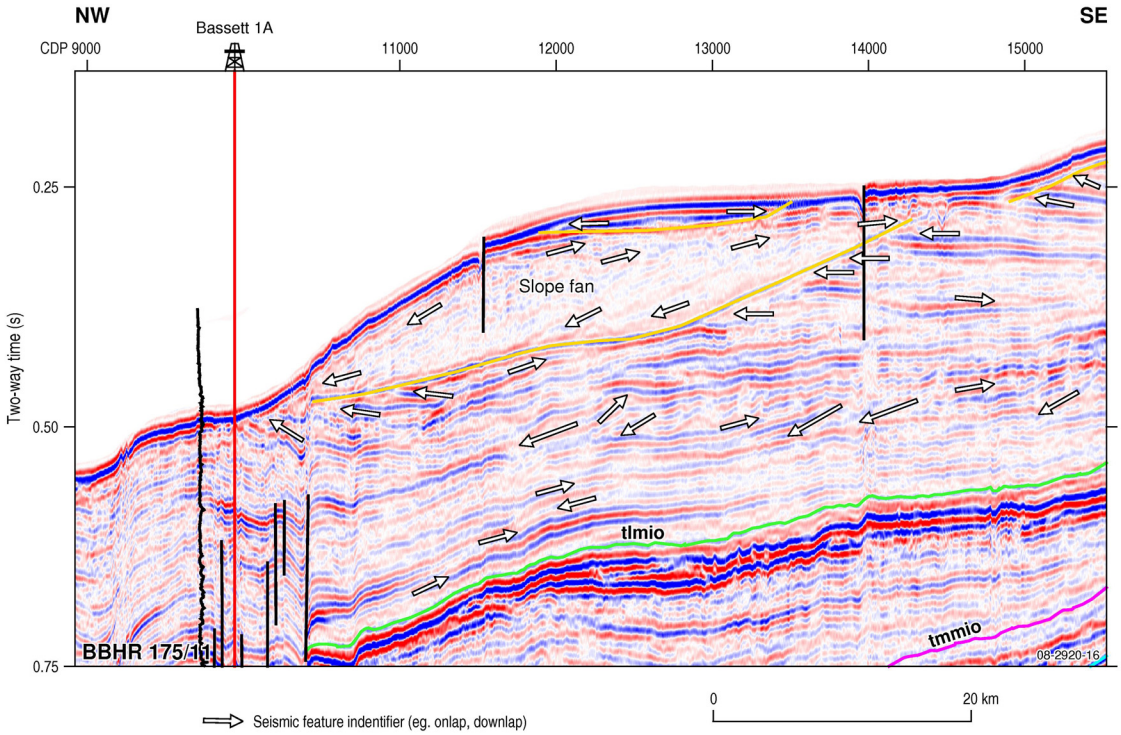

Figure 27: *BBHR 11. Seismic features of the Pliocene to Holocene period, including subtle progradation, an erosion surface followed by deposition of a slope fan.*

Conclusions

1. An apparent lack of Cenozoic deformation and the coincidence of the highest quality reservoir and seal pair indicate that the area with the highest potential in the Caswell Sub-basin for CO_2 storage within the Cenozoic sequence is located within the central Sub-basin near Caswell-2 and Walkley-1.
    - The sandstones in this area of the basin are thick and broad with good porosity and permeability and are situated well below supercritical depth.
    - The carbonates in this sub-basin have the lowest porosity values and the thickest sections. In addition, palaeogeographic reconstructions indicate that carbonates in this area did not have sustained aerial exposure during the Oligocene lowstand or Pliocene/Holocene lowstands. Thus, the probability of secondary porosity and karstic features occurring within these carbonates is lower than in carbonates in the eastern sub-basin that appear to have experienced fluvial and aerial erosion.
2. Cenozoic sandstones are spatially limited in the Browse Basin, with negligible Cenozoic sandstones encountered in the Barcoo Sub-basin and north-western Caswell Sub-basin.
3. MICP analysis suggests that the carbonate lithologies with the best seal potential are those with a high micrite component (mudstones and wackestones), whereas those with lower micrite components (packstones and grainstones) have relatively low seal capacity.
4. Deformation during the Cenozoic was extensive in the north-east Caswell Sub-basin, with significant faulting and associated subsidence of Cenozoic deposits. In some cases, faults are observed to penetrate the seafloor.
5. The gamma ray response alone is insufficient to differentiate between Cenozoic carbonates and sandstones in the Browse Basin, as grainstones and packstones typically have a similar gamma ray response to sandstone. Furthermore, whilst the sonic response does not show consistent

variation in response between clastic and carbonate deposits, it does provide insight into the lithological changes in the carbonates.

6. The characteristic seismic response of Cenozoic carbonates and sandstones in the Browse Basin is sufficiently distinct to allow differentiation of these two lithologies on seismic lines. The seismic impedance of the Cenozoic sandstones ranges from chaotic to moderately continuous and typically low to moderate amplitude reflections. In contrast, the carbonates typically show high continuity and moderate to high amplitude reflections.
7. An assessment of well completion reports in the Browse Basin and concomitant review of the BBHR report has revealed several key differences, including over 200 m in the stratigraphic boundaries as defined in well completion report and the BBHR report in Echuca Shoals-1, Discorbis-1 and Bassett 1a. Evaluation of BBHR seismic lines and wireline logs for each of the wells supports the position of the BBHR base Cenozoic marker in both Echuca Shoals-1 and Discorbis-1, but suggests that it may actually be lower within Bassett-1a.

Acknowledgements

We would particularly like to thank Alfredo Chirinos and Anna-Liisa Lahtinen for their patient response to our numerous questions during this project and for their review of the manuscript. We would also like to thank Rick Causebrook for his assistance in setting up this project and for his ongoing interest in our findings. In addition, the advice of Diane Jorgenson and her thoughtful review of this manuscript is much appreciated. Finally we appreciate the advice and help of Kane Rawsthorn during our project. To all of the above, your willingness to help whenever we needed it made this project an enjoyable learning experience.

We would also like to acknowledge Eddie Resiak and Paula Cronin for facilitating viewings of the cuttings and Richard O'Brien at the Department of Industry and Resources in Western Australia and Darryl Stacey at the Northern Territory Department of Primary Industry, Fisheries and Mines for their speedy response and approval of sampling permissions. Finally we would like to acknowledge Ric Daniels for MICP analysis.

Finally, we would like to acknowledge the time and careful thought that Aleks Kalinowski, Barry Bradshaw and Rob Langford put into the review of this manuscript.

References

AGSO Browse Basin Project Team, 1997. Browse Basin high resolution study, North West Shelf, Australia, Interpretation Report. *AGSO record* 1997/38.

Blevin, J.E., Struckmeyer, H.I.M., Cathro, D.L., Totterdell, J.M., Boreham, C.J., Romine, K.K., Loutit, T.S., Sayers, J., 1998. Tectonostratigraphic framework and petroleum systems of the Browse Basin, North West Shelf. *The Sedimentary Basins of Western Australia: Proceedings of Petroleum Exploration Society of Australia Symposium 2*, 369-395.

Bradshaw, B.E., and Bradshaw, J., 2000. Geodisc Project 1 – Regional Analysis; Browse Basin Pilot Study. *AGSO & Australian Petroleum Cooperative Research Centre*.

Bradshaw, J., and Rigg, A. J., 2001. The GEODISC Program: research into geological sequestration of CO_2 in Australia. *Environmental Geosciences* 8, 166-176.

Dunham, R. J., 1962. Classification of carbonate rocks according to depositional texture. In: Ham, W. E. (ed) *Classification of Carbonate Rocks.* American Association of Petroleum Geologists, Memoir 1, Tulsa Oklahoma, 108-121.

Hardenbol, J., Thierry, J., Farley, M.B., Jaquin, T., Graciansky, P.C. and Vail, P.R., (1998). *Mesozoic and Cenozoic Sequence Chronostratigraphic Framework of European Basins*. SEPM Special Publ. # 60, 8 charts

Stephenson, A. E. & Cadman, S. J., 1994. Browse Basin, Northwest Australia: the evolution, palaeography and petroleum potential of a passive continental margin. *Palaeography, Palaeoclimatology, Palaeoecology* 111, 337-366.

Struckmeyer, H.I.M., Blevin, J.E., Sayers, J., Totterdell, J.M., Baxter, K., Cathro, D.L., 1998. Structural evolution of the Browse Basin, North West Shelf; new concepts from deep seismic data. *The Sedimentary Basins of Western Australia: Proceedings of Petroleum Exploration Society of Australia Symposium 2*, 345-367.

Willis, I., 1988. Results of exploration, Browse Basin, North West Shelf, Western Australia. In: P.G. Purcell & R.R. Purcell (eds), *The North West Shelf, Australia*. Proceedings of Petroleum Exploration Society Australia Symposium, Perth, 259-272.

Wentworth, C. K., 1962. A scale of grade and class terms for clastic sediments, *Journal of Geology* 30**,** 377-392.

WELL COMPLETION REPORTS

Amoco Australia (1992). Arquebus 1 well completion report (unpublished).
Amoco Australia (1993). Sheherazade 1 well completion report (unpublished).
Ampolex (1993). Walkley 1 well completion report (unpublished).
BHP Petroleum (1987). Asterias-1 well completion report (unpublished).
BHP Petroleum (1987). Gryphaea-1 well completion report (unpublished).
BHP Petroleum (1988). Kalyptea-1 (first) well completion report (unpublished).
BHP Petroleum (1989). Discorbis-1 well completion report (unpublished).
B.O.C. Australia (1970). Lynher 1 well completion report (unpublished).
B.O.C. Australia (1971). Scott Reef 1 well completion report (unpublished).
B.O.C. Australia (1972). Rob Roy 1 well completion report (unpublished).
B.O.C. Australia (1974). Heywood-1 well completion report (unpublished).
B.O.C. Australia (1974). Lombardina 1 well completion report (unpublished).
B.O.C. Australia (1974). Prudhoe-1 well completion report (unpublished).
B.O.C. Australia (1974). Yampi 1 well completion report (unpublished).
ELF Aquitane Exploration Australia (1988). Delta 1 well completion report (unpublished).
Inpex Browse (2000). Dinichthys 1 well completion report (unpublished).
Mobile Exploration (1991). Productus-1 well completion report (unpublished).
Mobile Exploration (1993). Copernicus ST-1 well completion report (unpublished).
Norcen International (1992). Maret 1 well completion report (unpublished).
Santos Limited (1986). Browse Island 1 well completion report (unpublished).
Shell Development (1990). Buccanneer-1 well completion report (unpublished).
Shell Development (1991). Trochus 1 well completion report (unpublished).
Shell Development (1998). Adele-1 well completion report (unpublished).
Woodside Petroleum (1978). Bassett-1A well completion report (unpublished).
Woodside Petroleum (1977). Scott Reef 2A well completion report (unpublished).
Woodside Petroleum (1980). Barcoo 1 well completion report (unpublished).
Woodside Petroleum (1980). Brecknock-1 well completion report (unpublished).
Woodside Petroleum (1980). Buffon-1 well completion report (unpublished).
Woodside Petroleum (1981). Brewster 1A well completion report (unpublished).
Woodside Petroleum (1982). North Scott Reef 1 well completion report (unpublished).
Woodside Petroleum (1983). Caswell 2 well completion report (unpublished).
Woodside Petroleum (1983). Echuca Shoals-1 well completion report (unpublished).

Appendices

A1. Summary of the Cenozoic sequence in wells of the Browse Basin, as determined from well completion reports. **See CD-ROM**

A2. Descriptions of well cuttings from the Cenozoic section of Discorbis-1, Caswell-2, Echuca Shoals-1, Copernicus-1 and Bassett 1a. **See CD-ROM**.

A3. Photomicrographs of cuttings of the Cenozoic section of Discorbis-1, Caswell-2, Echuca Shoals-1, Copernicus-1 and Bassett 1a. **See CD-ROM**.

A4. Electronic Copy of the MICP report and XRD analysis. **See CD-ROM**

A5. Print out of Gamma Ray and Sonic logs in the Cenozoic section of Discorbis-1, Caswell-2, Echuca Shoals-1, Copernicus-1 and Bassett 1a together with basic lithological interpretation. **See CD-ROM**

A6. Summary of sandstone porosity information available within Browse Basin well completion reports

A7. XRD Results

Appendix A6. Summary of sandstone porosity information available within Browse Basin well completion reports

WELL	DEPTH (m)	AGE	LITHOLOGICAL DESCRIPTION	VISUAL POROSITY ESTIMATIONS	LOG POROSITY ESTIMATIONS
Gryphaea-1	1212-1247	Miocene to Recent	Sandstone	>30%	
	1466-2000	Eocene/Paleocene	Sandstone	23 - 30 (in sands)	
Asterias-1	1272-1465	Eocene/Paleocene	Sandstone	Varies from good to moderately poor in many of the aggregates	
	1465-1495	Eocene/Paleocene	Interbedded Sandstone	Good visible porosity	
	1558-1587	Eocene/Paleocene	Interbedded Sandstone	Poor visible porosity	
	1624-1627	Eocene/Paleocene	Sandstone	Good visible porosity	
	1914-1936	Paleocene	Siltstone	Poor to occasionally moderate porosity	
Productus-1	773-1011	Early-Middle Eocene	Upper interval: calcarenite & fossiliferous quartzose sandstone; middle int.: quartzose sandstone; lower int.: calcilutite.	Good inferred porosity in sandstone. Some place have nil-good inferred porosity; 850m - 950+ has v good to excellent inferred porosity; 970+ has nil to poor visual porosity.	
	1088.8-1152.2	Paleocene	Sandstone & interbedded argillaceous sandstone	Porosity is very good to excellent (poor in interbedded argillaceous sandstones); 1090m+: fair to very good inferred porosity; 1030m+: very good inferred porosity.	
Copernicus	1065-1136	Middle-Early Eocene	Sandstone	Poor to occasionally fair visual porosity	
	1229-1352	Paleocene	Sandstone	Poor to occasionally fair visual intergranular porosity	
Bassett-1a	1120-1345	Indeterminable	Sandstone	Very good visual intergranular porosity	1120-1455m logged as 22-35%.
	1345-1415	Indeterminable	Sandstone	Trace to poor visual intergranular porosity	1120-1455m logged as 22-35%
	1415-1455	Indeterminable	Sandstone	Fair visual intergranular porosity	SW Core 1432=%15 intergranular; 1120-1455m log 22-35%.

WELL	DEPTH (m)	AGE	LITHOLOGICAL DESCRIPTION	VISUAL POROSITY ESTIMATIONS	LOG POROSITY ESTIMATIONS
	1481-1520	Indeterminable	Sandstone	Poor to good visual intergranular porosity	1455-1833m logged as 9-35%.
	1520-1625m	Indeterminable	Sandstone	Very good visual intergranular porosity	SW Core: 1542m=20% intergranular; 1574.5m=25% intergranular; 1595.5m=15% intergranular; 1455-1833m logged as 9-35%.
Bassett-1a	1625-1832	Indeterminable	Sandstone	Fair to very good visual intergranular porosity	SW Core: 1665m=20% intergranular; 1690m=20% intergranular; 1708.5m=20% intergranular; 1723.5m=Trace intergranular; 1735.5m=5% intergranular; 1770m=20% intergranular; 1796.5m=Trace intergranular; 1800.5m=15% intergranular; 1803.5m=10% intergranular; 1829m=10% intergranular; 1455-1833m logged as 9-35%.
	1840-2005	Paleocene	Sandstone	Very good visual intergranular porosity	SW Core: 1862m=15% intergranular; 1870m=20% intergranular; 1884m=10% intergranular; 1906.5m=15% intergranular; 1943.5m=15% intergranular; 1952m=25% intergranular; 1968m=Trace intergranular; 1987.5m=20% intergranular; 1996.5m=Trace intergranular; 1943-2020m logged as 25-30%.
Heywood-1	882-1590	Eocene	Sandstone	Dominantly very good porosity (>35%)	
Adele-1	910-925	N/A	Sandstone	Inferred good porosity	
	945-1170	N/A	Sandstone	Inferred good porosity	
	1170-1255	N/A	Sandstone	Inferred very good porosity	
	1310-1505	N/A	Sandstone	Inferred very good porosity	
	1505-1605	Early Eocene	Sandstone	Poor to good intergranular porosity	
	1605-1650	N/A	Sandstone	Inferred very good porosity	
Echuca	791-800	Miocene - Eocene	Sandstone	Good	30-45%
Shoals-1-1	840-1614	Eocene – Paleocene	Sandstone	Fair to good porosity	920-1347m: 20-47%, 1347-1770m: 25-45%
Prudhoe-1	750-785	Middle Miocene to Burdigalian	Sandstone	Poor to very good visual porosity	
	816-1208	Eocene	Sandstone	Good to very good visual porosity (20-25% visual porosity)	
	1208-1330	Eocene/Paleocene	Sandstone	Good to very good visual porosity (20-25% visual porosity)	

WELL	DEPTH (m)	AGE	LITHOLOGICAL DESCRIPTION	VISUAL POROSITY ESTIMATIONS	LOG POROSITY ESTIMATIONS
Brewster-1	1018-1275	Late - Mid-Miocene	Sandstone	Good intergranular porosity (visual 15-25%)	20-40%
	1285-1465	Late to Mid-Eocene	Sandstone	Good intergranular porosity (visual 5-25%)	
	1465-1555	Paleocene	Sandstone	Good intergranular porosity (visual 5-25%)	
	1555-1628	Paleocene	Sandstone	Good intergranular porosity (visual 5-25%)	
Rob Roy-1	427-567	Miocene to Pliocene	Interbedded Sandstone	Poor to good intergranular porosity.	
	567-700	Paleocene	Sandstone	Good intergranular porosity to poor-fair intergranular porosity	Average sonic porosity 51%
Caswell-2	1660-1952	Middle Eocene?	Sandstone		5 - 45%
	2079-2473	Undifferentiated Middle Eocene	Sandstone		8 – 37%
	2473-2595	Paleocene	Sandstone		8 – 37%
Walkley-1	1608.4-1770	Palaeogene	Sandstone	Good to excellent visible intergranular porosity in sandstone, poor to fair visible porosity in aggregates;	
	1770-1795	Palaeogene	Calcareous Sandstone	Poor to very good visible intergranular porosity in sandstone; Poor inferred porosity in calcarenite.	
	1959.5-1979	Palaeogene	Interbedded Sandstone	Poor-fair visual interparticle porosity in calcarenite; Fair-good visible intergranular porosity in sandstone.	
	1979-2213	Undifferentiated Paleocene-Eocene	Sandstone	Poor-good visible intergranular porosity in Sandstone. Poor-fair visible intergranular porosity in glauconitic Sandstone.	
	2213-2385	Undifferentiated Paleocene-Eocene	Sandstone	Fair-good visible intergranular porosity in sandstone. Poor-fair visible intergranular porosity in glauconitic sandstone.	
Yampi-1	408-545	Pliocene to Middle Miocene	Sandstone	Good visible intergranular porosity (5-25% intergranular porosity)	
	779-789	Lower to Mid-Miocene	Interbedded Sandstone	Good visual porosity (15% intergranular porosity)	
	789-824	Eocene?	Sandstone	Good visual porosity	
	824-942	Eocene?	Sandstone	Very good visual porosity (10 - 15% intergranular porosity)	
	942-1014	Paleocene	Sandstone	Very good visual porosity (25% intergranular porosity)	
Lynher-1	293-426	Upper Paleocene to Eocene	Sandstone	Soft trace intergranular porosity above 329 m and below 415 m, otherwise no effective porosity.	

A7. XRD Results showing minerals present in selected samples and the corrected weight as a percentage of the sample

WELL	CASWELL-2	DISCORBIS-1	DISCORBIS-1	ECHUCA SHOALS-1	ECHUCA SHOALS-1
SAMPLE DEPTH	1950m	2046m	2349m	1355m	1365m
GEOSCIENCE AUSTRALIA SAMPLE NUMBER	1937555	1937556	1937557	1945758	1945759
QUARTZ	54.3	34.1	52.5	84.8	94.1
DOLOMITE	24.5	35.8	43.5		
CALCITE	17.5	11		6	
KAOLIN	2.4	1.5			
SODIUM CHLORIDE	1.3	0.9	0.6	2.5	1.3
MICROCLINE	0.1	1.9			
ANKERITE		14.8			
MUSCOVITE			3.4		
GYPSUM				5	3.6
PYRO-PHYLLITE				1.7	1.1
TOTAL %	100.1	100	100	100	100.1

Instructions for the CD-ROM

Description, Distribution and Potential CO_2 Storage/Seal Capacity of the Cenozoic Sandstones and Carbonates, Browse Basin, Western Australia

This CD-ROM contains the above-titled Report as Record 2008/13.pdf

View this .pdf document using Adobe Acrobat Reader (click Adobe.txt for information on readers)

Click on: Record 2008/13.pdf to launch the document.

Directories on this CD-ROM:

- **A1. Summary of the Cenozoic sequence in wells of the Browse Basin, as determined from well completion reports.**
- **A2. Descriptions of well cuttings from the Cenozoic section of Discorbis-1, Caswell-2, Echuca Shoals-1, Copernicus-1 and Bassett 1a..**
- **A3. Photomicrographs of cuttings of the Cenozoic section of Discorbis-1, Caswell-2, Echuca Shoals-1, Copernicus-1 and Bassett 1a.**
- **A4. Electronic Copy of the MICP report and XRD analysis.**
- **A5. Print out of Gamma Ray and Sonic logs in the Cenozoic section of Discorbis-1, Caswell-2, Echuca Shoals-1, Copernicus-1 and Bassett 1a together with basic lithological interpretation.**